FACULDADE DE ENGENHARIA DA UNIVERSIDADE DO PORTO

Biomechanical analysis of the influence of a cholesteatoma in human hearing

Maria Leonor Illa Mendonça

DISSERTATION

Integrated Master in Bioengeneering

Supervisor: Carla Bibiana Monteiro França Santos | PhD

Co-supervisors: Professor Maria Fernanda Gentil Costa
Professor Marco Paulo Lages Parente

July 2020

Biomechanical analysis of the influence of a cholesteatoma in human hearing

Maria Leonor Illa Mendonça

Integrated Master in Bioengeneering

July 2020

Resumo

O sistema auditivo humano é um sistema complexo, com estruturas particulares que possibilitam a audição. O ouvido médio, estudado em detalhe nesta tese, é formado por uma cavidade na qual existe uma cadeia ossicular articulada de modo a transferir mecanicamente as informações sonoras desde a membrana timpânica até ao ouvido interno, onde a informação é codificada e enviada para o cérebro, para interpretação. Além dos ossículos, músculos e ligamentos a eles conectados, há outra estrutura importante que atravessa o ouvido médio, o nervo da corda timpânica. Este nervo é uma ramificação do nervo facial, estando associado ao paladar e à produção de saliva. Esticar ou pressionar este nervo pode causar lesões permanentes nesta estrutura, levando à paralisia facial. Apesar de a sociedade ser inclusiva, as pessoas com paralisia facial podem sofrer alguns constrangimentos. As doenças do ouvido médio podem comprometer o funcionamento da corda do tímpano, ao esmagá-la, e a capacidade auditiva, reduzindo as vibrações da cadeia ossicular, o que resultará em menos informação a chegar ao ouvido interno. Uma dessas doenças é otite média. Se não for bem tratada, e caso dure mais de 3 meses, esta doença pode evoluir para um estado crónico, havendo maior probabilidade de desenvolvimento de um colesteatoma, uma massa benigna feita de detritos de pele. Nesta dissertação, estudou-se a influência do desenvolvimento do colesteatoma próximo da corda timpânica, de forma a avaliar as consequências dessa massa na audição e possível paralisia facial. Assim, foi utilizado um modelo do ouvido previamente desenvolvido, baseado no método dos elementos finitos. O modelo foi aprimorado através da modelação e adição da corda timpânica. Três colesteatomas de tamanhos diferentes foram criados na articulação entre o martelo e a bigorna e adicionados ao modelo. Um nível de pressão sonora de 60 e 80 dB SPL foi aplicado na membrana timpânica e realizou-se uma análise em estado estacionário para frequências de 100 Hz a 10 kHz. Para avaliar o impacto na função auditiva, foram analisados os deslocamentos da membrana timpânica e da base do estribo. Os resultados foram comparados com um caso saudável, sem tumor no ouvido médio. Foi demonstrado que o desenvolvimento de um colesteatoma leva a uma diminuição dos deslocamentos tanto no início como no fim da cadeia ossicular. Foram também realizados alguns testes atribuindo propriedades semelhantes aos ossículos ao tumor maior, já que os tumores se tornam em estruturas rígida e densas ao longo do tempo. Este caso levou a uma diferença ainda maior em termos de deslocamento. Além disso, como os colesteatomas são capazes de recrutar osteoclastos que degradam osso, a degradação dos ossículos também foi simulada. Os deslocamentos observados mostram uma diminuição considerável para o tumor maior. A fase da resposta do deslocamento foi também comparada para todas as situações estudadas. As diferenças de deslocamento observadas estão diretamente relacionadas com a perda auditiva, sendo possível concluir que o crescimento de um colesteatoma no ouvido médio levará a problemas auditivos. A influência do crescimento tumoral na corda timpânica foi também analisada. As tensões no nervo foram avaliadas em dois momentos: quando o tumor interage com ele pela primeira vez, empurrando-o para baixo, e quando o tumor o esmaga contra a bigorna. As tensões obtidas permitiram inferir sobre as consequências a nível do paladar e da paralisia facial, embora alguns estudos relatem que, quando a pressão diminui, é possível recuperar totalmente.

Abstract

The human auditory system is a complex system, with particular structures that play important roles, turning hearing possible. The middle ear, further explored in this dissertation, consists of a cavity filled with an ossicular chain articulated to mechanically transfer the sound information from the tympanic membrane to the inner ear, where the information is coded, being afterwards sent to the brain for interpretation. Besides the ossicles, muscles and ligaments attached, there is another important structure crossing the middle ear, the chorda tympani nerve. This nerve is one of the facial nerve branches, being associated to taste sensation and saliva production. Stretching or pressuring this nerve may cause injuries in this structure, that may result in permanent damage leading to facial paralysis. Despite the society being inclusive, people with facial paralysis may suffer some constraints. Diseases in the middle ear may compromise chorda tympani functioning, due to its pinching, as well as hearing ability, by reducing the vibrations in a certain point of the ossicular chain, which will result in a poor information reaching the inner ear. One of this conditions is otitis media. If this disease is not properly treated and lasts for more than 3 months, it may develop to a chronic otitis media. In this case, appearance and growth of a cholesteatoma, a benign mass made of skin debris, have higher probability. In this dissertation, the influence of cholesteatoma development near chorda tympani nerve was studied, in order to assess the consequences of this mass in both hearing and possible facial paralysis. To do so, a previously developed ear model based on the finite elements method was used. The model was improved by modeling and adding the chorda tympani nerve to it. Three different sized cholesteatomas were created in the connection between the malleus and the incus and assembled to the model. A sound pressure level of 60 and 80 dB SPL was applied in the tympanic membrane and a steady state analysis was performed for frequencies from 100 Hz to 10 kHz. To assess the impact on hearing function, the displacements of the tympanic membrane and of the stapes footplate were analysed. The results were compared with a healthy case, where no tumour existed in the middle ear. It was shown that the cholesteatoma development leads to a decrease in the displacements both at the beginning as well as at the end of the ossicular chain. Some tests were also performed assigning the larger tumour properties similar so the ossicles, as tumours become harder and denser structures along time. This case led to an even greater displacement difference. Furthermore, as cholesteatomas are able to recruit osteoclasts that degrade bone, the ossicles degradation was also simulated, by assigning tumour properties to part of the ossicles. The observed displacements show a considerable decrease for the larger tumour in these conditions. The phase angle of the displacement was also compared for all the studied situations. The observed displacement differences are directly connected to hearing loss, being possible to conclude that cholesteatoma growth in the middle ear will lead to hearing problems. The influence of tumour growth on chorda tympani nerve was also analysed. The tensions felt in this nerve were assessed in two moments: when the tumour first interacts with it, pushing it down, and when the tumours squeezes it against the incus. The obtained tensions allowed to infer on the consequences regarding taste disturbance and facial paralysis, although some studies report that when pressure fades away, it is possible to fully recover.

Agradecimentos

Em primeiro lugar, quero deixar o meu sincero agradecimento à minha orientadora, Dra. Carla Santos, por toda a ajuda, por ser incansável e por ter sempre uma palavra motivadora. Muito obrigada pela sua disponibilidade. Foi um gosto trabalhar consigo.

Aos meus co-orientadores, Prof. Dr. Marco Parente, por todo o apoio e ajuda na resolução de problemas durante o desenvolvimento deste trabalho. A sua ajuda foi essencial para a realização desta tese, muito obrigada! E à Prof. Dra. Fernanda Gentil, por me ajudar e orientar em toda a parte clínica associada a este trabalho. Muito obrigada por todas as sugestões e conselhos! E agradecer também ao Prof. Dr. Renato Natal, que se manteve sempre por perto, contribuindo com importantes dicas para o sucesso deste projeto.

A toda a minha família, um grande obrigada por me manterem motivada ao longo de todo o meu percurso académico. Por manterem a vossa expectativa alta, levando-me sempre a querer fazer mais e melhor. Um agradecimento especial aos meus pais e às minhas irmãs, por nunca se cansarem de todas as minhas queixas e desabafos (ou cansarem, mas continuarem a aturá-los :)).

Aos professores que me acompanharam ao longo dos vários anos escolares, com especial destaque para a professora Adélia, o professor Luís, a professora Susana e o professor Jorge. Obrigada por me inspirarem e motivarem! Se esse é o papel de um professor, no que me diz respeito, a missão foi cumprida.

A quem verdadeiramente me acompanhou nestes 5 anos. Raquel, obrigada por estares sempre lá e seres a minha fiel companheira (e gémea, como muitos dizem) nesta jornada. Bruno, por todas as vezes em que reclamamos sobre tudo e por teres sempre as ideias mais fora da caixa. Pedro, Pedrão e Migas, por serem muito bons a criticar quando é preciso, mas serem também os melhores compinchas que podia ter ao longo destes anos. Um obrigada ao Luís e à Leonor, génios incompreendidos em Bio, mas que não conseguem cortar as raízes a este curso maravilhoso. E claro, aos preferidos ainda não mencionados (sem nenhuma ordem específica, para não ferir os mais sensíveis), Meneses, por todos os áudios e pela incrível energia que transmites ao grupo, Álvaro, por permitires que o nível de português e o nível de piada do grupo sejam inversamente proporcionais, Joana e Natália, por serem as melhores e mais adoradas biotecas com espírito biomédico, Gu, por seres, juntamente com o 3D, um dos grandes responsáveis por biomédica ser um grupo de amigos e não de colegas e Ana, por seres também um elemento essencial nesta difícil tarefa, sempre com ideias de eventos e atividades incríveis. A todos muito obrigada pela forcinha, videochamadas e mensagens diárias. Sem vocês não teria sido a mesma coisa.

A amizades que já têm uns aninhos. Raquel, por seres a minha confidente e me apoiares sempre! Catarina, por saber que posso sempre contar contigo! Kika, por nos termos aventurado juntas nesta loucura que é a Bioengenharia e por todas as boas histórias. Ao Picão, Luisinho, Bea, Matilde, Marta, Rodrigo, Bárbara e Gonçalo. Obrigada a todos por se manterem presentes.

Uma menção especial a quem, nos últimos 3 anos, me fez descobrir uma grande paixão. Sofia e toda a equipa Barquinho, obrigada por serem o espaço em que sempre me senti realizada! Quem diria que o que eu pensava que seria "apenas um part-time" me poderia trazer tanto. Não encarei

como trabalho nem um dia que fosse. Obrigada por acreditarem em mim e por me apoiarem sempre! (E um grande agradecimento aos meus alunos, que são os melhores do mundo!)

And of course, Mireia, Charlotte D, Charlotte B, Katelynn, Belisa, Monica and Eva, thanks for all the good memories in Groningen! Erasmus would not have been the same without you girls!

Por fim, agradecer a todas as pessoas relacionadas com a dança que tiveram impacto na minha vida, por partilharmos juntos esta paixão. E uma menção especial à Raquel, por ser a minha boleia oficial para todos os eventos e por todas as memórias partilhadas.

A todos... muito obrigada!

Leonor Mendonça

"Não tenhamos pressa, mas não percamos tempo."

José Saramago

Contents

List of Figures

List of Tables

Abbreviations and Symbols

AOM	Acute Otitis Media
COM	Chronic Otitis Media
CT	Computed Tomography
CTN	Chorda Tympani Nerve
FEM	Finite Elements Method
FP	Facial Palsy
MRI	Magnetic Resonance Imaging
OM	Otitis Media
SPL	Sound Pressure Level
TM	Tympanic Membrane
WHO	World Health Organization

Chapter 1

Introduction

1.1 Motivation

The ear is an important human organ, having essential functions in the day-to-day life. Responsible for one of the five human senses, it is a valuable system, used to grasp stimulus and information that surround people everyday. The ear is then of the utmost importance for a daily well-being.

Considering that the human body is such a complex system, some disorders may occur. Diseases associated to the auditory system may result in hearing loss or other nefarious consequences. Otitis media, an inflammatory disease of the middle ear, is a common illness of the auditory system. If this inflammation becomes chronic, it can lead to the development of a cholesteatoma, a benign ear tumour. This mass can appear in several locations, interfering with the regular functions of the internal ear structures, leading to hearing problems. If it grows in such a site that pressures the chorda tympani nerve (CTN), as one of the facial nerve branches that crosses the ear ossicular chain in the middle ear, it can result in facial palsy (FP), the inability to move a part of the face. Tumour development around this area can cause lesions that may be irreparable.

Hearing loss and FP can bring adaptation problems. Patients suffering from this condition would greatly benefit from a study to evaluate the risk and influence of the presence of different sized tumours in the middle ear as well as these bodies pressuring the CTN. Therefore, a study on the effect of tumour growing in the surroundings of this nerve is of major interest and pertinence. The results of this work may be used to better understand this, leading to further studies on the best approaches to treat this condition or minimize its effects.

1.2 Context

The human ear is the organ responsible for hearing and equilibrium. The peripheral auditory system can be divided into external, middle and inner ear, subsystems that work together with the same final goal. In spite of the well established coordinated functioning of the ear structures, several types of diseases can occur in the ear, compromising its behaviour. Otitis media (OM) is

an infection in the middle ear, being one of the most frequent conditions associated to this organ [1]. This disease can include the appearance of fluid in the middle ear and it can present itself as acute, associated with intense pain and lasting one to two weeks, or, if it lasts for more than three months, chronic, leading to the creation of the necessary conditions to hearing loss and tumour development.

Cholesteatoma is the most frequent type of tumour that can result from chronic otitis media (COM), being composed of an accumulation of skin debris [2]. Although this mass is usually a benign tumour, its surveillance is very important, since it grows and wears out the surrounding structures [3].

The effect of benign tumours on different sites of the middle ear was already a matter of study before, by Savaris et al., in the scope of the investigation in which this project is inserted [4]. Tumours connected to the incus, stapes and the medial surface of the tympanic membrane (TM) were simulated and their effects were analysed. Depending on its size and location, these tumours can affect the ear function in several ways. However, there is no study on the influence of a cholesteatoma that pressures the CTN. This structure is a facial nerve branch that is directly involved in the taste sensation of the anterior two thirds of the tongue as well as saliva production. The growth of these tumours between the malleus and the incus may pressure the CTN, causing ultimately FP. According to Ikeda et al., this problem can only be completely reverted if it is treated while the nerve is under pressure but has not suffered lesion, otherwise there is no full recovery [2]. This way, a study on the influence of these tumours in the CTN would be helpful to better understand the relation between the size and location of the tumour and the effects on hearing and on the nerve itself.

1.3 Goals

The goal of this work is to study the consequences of the growth of a cholesteatoma near CTN in what concerns hearing function and FP. With this in mind, Finite Element Method (FEM) will be used to simulate the desired conditions. A computational ear model has already been developed in former projects and will be used in this work. This model consists of TM, middle ear ossicles, ligaments and tendons, cochlear fluid, involving temporal bone, skin and ear cartilage, jaw and air in the external auditory canal and tympanic cavity. However, the CTN itself is not modeled yet. Thus, the CTN must be constructed and incorporated in the existing model. After that, different sized tumours associated to the ossicular chain will be simulated. The area of interest is the connection between the malleus and the incus, since that is the location of the middle ear crossed by CTN. The effects of the tumour growth around the CTN will be studied, in order to better understand for which tumour sizes the CTN is under pressure and from which tumour dimensions injuries in CTN occur.

Tumour resection is a delicate process and it should be performed as early as possible, since cholesteatomas wear out the structures to which they are connected to. This way, when applying pressure in the CTN, these masses will also erode this nerve. Thus, this project aims to evaluate

the consequences of this condition in order to better understand it and so that, in the future, further studies can be conducted to avoid middle ear structures damage.

Overall, this dissertation is relevant to allow a better comprehension of CTN and its position in the human body, as well as the influence of a cholesteatoma in human hearing and the consequences of pressuring this nerve.

1.4 Expected Contribution

In this project, the CTN structure was modeled. This model was added to the current ear biomechanical model, contributing to a more complete and accurate model. After this, the effects of cholesteatoma growth associated to the ossicle chain on hearing were assessed. Additionally, the influence of the appearance and development of a cholesteatoma in CTN surroundings was studied, providing more information on this structure as well as its weaknesses.

It is possible to summarize this project main contributions as:

- Computational development of an ear structure and biomechanical analysis of its behaviour,
- Better knowledge and study of CTN,
- Study of the effects of tumour (cholesteatoma) development in the surroundings of CTN regarding hearing and facial repercussions.

1.5 Structure

This dissertation is organized in five chapters. It starts with an introduction, where motivation and context, as well as main goals and expected contributions are presented.

Chapter 2 includes the anatomy and physiology of the auditory system with the main focus being CTN. Some middle ear pathologies are also described, with focus on OM and consequent cholesteatoma development. Finnaly, some works on CTN and cholesteatoma development are presented as well as the current biomechanical model of the ear and some previous related projects.

The followed methodology is presented in Chapter 3 and the results and their discussion in Chapter 4.

In the end, some conclusions are reached and future work is proposed.

Chapter 2

The ear

The human ear is a complex biomechanical system that plays an essential role in people's lives. In spite of much information being captured by the eyes, a lot of content is only perceived by the auditory system. Hearing is then an important skill to perform daily activities.

The ear is capable of tracking air pressure variations, connected to sound waves propagation, and transform them into electrical variations to be identified by the brain. It is responsible for both hearing and balance.

2.1 Anatomy and Physiology

The auditory system is located in the temporal bone and it can be divided in central auditory system and peripheral auditory system.

The central auditory system is formed by both the auditory nerve and auditory cortex. The peripheral auditory system can be split into three subsystems: external, middle and inner ear, as presented in Figure 2.1, with specific functions, that will be detailed next.

2.1.1 External Ear

The external ear is the most outer part of the ear and it goes from the atrium up to the TM, also called eardrum. When sound waves reach the external ear, they proceed through the external auditory canal. This canal has different properties along itself. Its most outer third part is fibrocartilaginous while the two internal thirds are made out of bone. This is important as the fibrocartilaginous part is covered by skin and one of the skin's layers, the dermis, is responsible for cerumen production, which avoids the passage of foreign bodies.

In the end of the external auditory canal there is the TM. Sound waves cause the vibration of the TM, making sound information follow to the next phase, the propagation in the middle ear. The TM is capable of transforming sound energy into mechanical energy. This membrane is a circular structure that can be split into *pars tensa* and *pars flaccida*. It has three tissue layers. The most external one is connected to the external auditory canal coating, being a thin layer. The inner layer is formed by epithelial tissue and connected to the middle ear coating. The portion

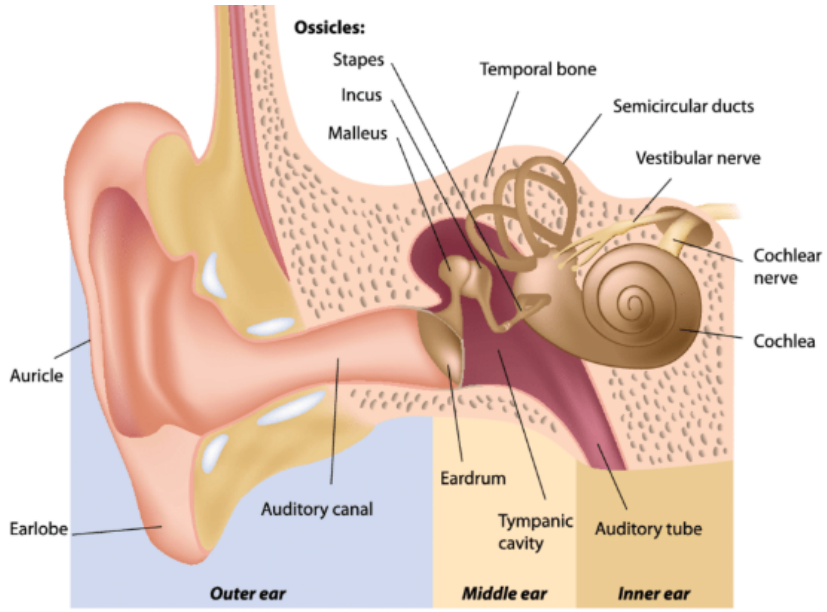

Figure 2.1: Representation of the human ear [5].

standing between these two layers is the one responsible for this structure function, being fibrous, with radial, parabolic and transverse fibers [6]. This layer holds the TM, providing it its vibratory ability. *Pars flaccida* has a low fibers content, as it only includes the internal and external layers, which explains its softness, while *pars tensa* has all three layers, being firm and elastic. The umbo is a salient part on the medial side of this membrane, connected to the malleus extremity [6].

2.1.2 Middle Ear

The middle ear is composed by the tympanic box, formed by the ossicular chain and the tympanic cavity. This part of the ear is filled with air, being the Eustachian tube responsible for the middle ear ventilation. The ossicular chain is formed by three small bones named ossicles that can be seen in Figure 2.2. The one that contacts with the TM is the malleus. This ossicle can be divided into head, neck, anterior and external apophysis and manubrium. The malleus neck is connected to the TM *pars flaccida* and the manubrium to the superior part of the TM, dragging it inwards. In the anterior apophysis there is the insertion of tensor tympani muscle. The malleus mass varies between 23 and 27 mg and its length between 7.6 to 9.1 mm [6, 7, 8, 9, 10]. The head of the malleus articulates with the next ossicle, the incus, which is formed by its body and three apophysis, long, short and lenticular. It is the only ossicle that is not connected to a muscle, being the heaviest of the three ossicles [6]. Its mass can go from 25 to 32 mg [7, 9]. Incus lenticular apophysis articulates with the stapes, the most internal and smallest ossicle, with only around 2 mg mass and 2.5 to 4 mm length [10]. It can be divided into head, neck, footplate and two crus, anterior and posterior, that connect the neck to the footplate. The posterior crus has a broader curvature than the anterior. In the posterior part of the neck there is the insertion of the stapedius muscle. The footplate is connected to the inner ear through the oval window.

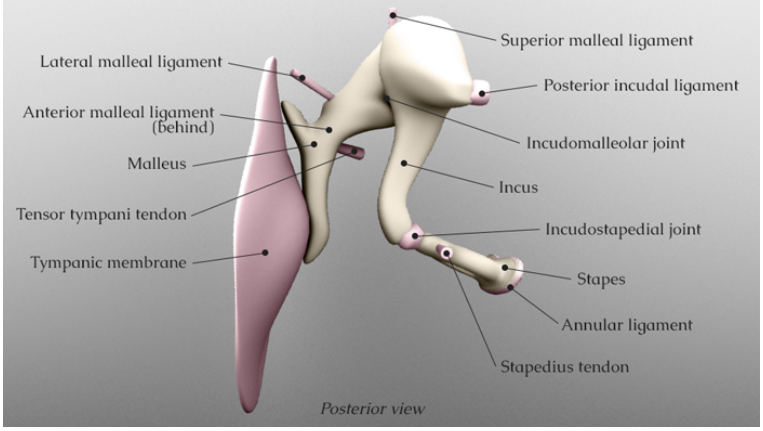

Figure 2.2: Middle ear ossicular chain representation [1].

As mentioned during the ossicles description, two muscles connected to these ossicles exist, tensor tympani and stapedius, being their main function to damp excessively loud noises.

Tensor tympani is a muscle located in the bony canal above the Eustachian tube that is inserted in the anterior apophysis of the malleus. It is innervated by the V cranial nerve (trigeminal nerve). Its main function is to damp loud sounds, like chewing or shouting. When under tension, this muscle pulls the malleus medially. This will lead to tension in the TM, causing the damping of vibration in the ossicles and thereby reducing the perceived amplitude of sounds [11].

The stapedius is the smallest skeletal muscle in the human body, being innervated by the VII cranial nerve (facial nerve). Its main functions are to stabilize the stapes and to reduce the pressure in the inner ear. This muscle controls sound waves intensity, protecting the inner ear. This is called esteatoacoustic reflex. People with injuries in stapedius muscle can develop hyperacusia, less tolerance to regular sounds.

Damping is more effective for low frequency sounds. Damages caused by sudden noises are hard to avoid, since the reflex is not fast enough. The articular surfaces of the ossicles are covered with cartilage, in order to avoid producing noise when moving. The same happens for the connection between the stapes footplate and the oval window.

The middle ear ossicles are hanging through six ligaments. Three of them are attached to the malleus (superior, anterior and lateral), two to the incus (posterior and superior) and one to the stapes (annular). In Figure 2.3 it is possible to see the mentioned muscles as well as some of the ligaments.

Also in the middle ear there is the CTN, a nerve that crosses the tympanic cavity between the malleus and the incus. This structure is described in detail in Section 2.1.2.1.

[1] Middle ear anatomy, Author:Skalski, Matt https://radiopaedia.org/images/30697108 Accessed on: 2020-01-29

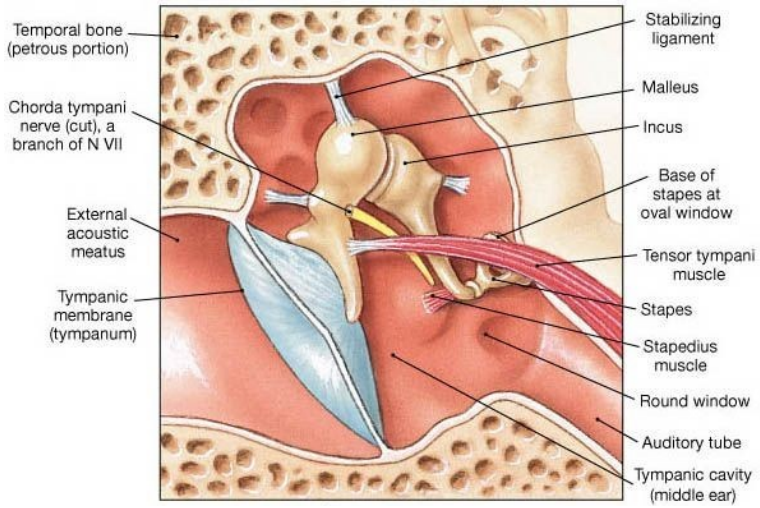

Figure 2.3: Middle ear muscles and CTN localization.

2.1.2.1 Chorda Tympani Nerve

The facial nerve arises from the brainstem proceeding to the facial area of the fundus of the internal acoustic meatus, finally entering the geniculum of the facial canal [12, 13]. It is responsible for the command of the muscles related to facial expression, for the external ear sensitivity, for fiber transportation for submandibular and sublingual glands and also for taste sensation in the anterior two thirds of the tongue.

This nerve has two paths, an intratemporal and an extratemporal one. The intratemporal segment can be divided into three parts, labyrinthic, tympanic and mastoid. The first corresponds to the facial nerve portion that passes inside the inner auditory canal. When it reaches the geniculate ganglion, the greater petrosal nerve arises, proceeding its way to innervate the lacrimal gland. The tympanic part, that has around 8 to 11 mm, starts in the geniculate ganglion, where the nerve bends around 40 to 80 degrees, proceeding through the tympanic segment until reaching the lateral semicircular canal. The nerve to stapedius, nerve that is related to the stapedius muscle, emerges from this part of the facial nerve. Finally, the mastoid segment has a 90 degrees curvature and goes down until the stylomastoid foramen, proceeding to the parotyd gland. From this point on, the extratemporal path of the facial nerve begins. In the parotid gland, the nerve splits into several branches, temporal, zygomatic, buccal, mandibular and cervical. This branch network is known as *pes anserinus* [15, 16, 17].

CTN, the structure of interest in the present work, is one of the facial nerve branches. According to Henry Gray, CTN arises from the facial nerve, around 6 mm above the stylomastoid foramen [18]. The course of CTN can be divided into three portions, as it is shown in Figure 2.4. The first portion, from the connection with the facial nerve to the tympanic cavity, is found in the mastoid process. The central section crosses the tympanic cavity. The final segment is located in the submandibular fossa and it goes from the tympanic cavity to the connection with the lingual nerve [15, 14].

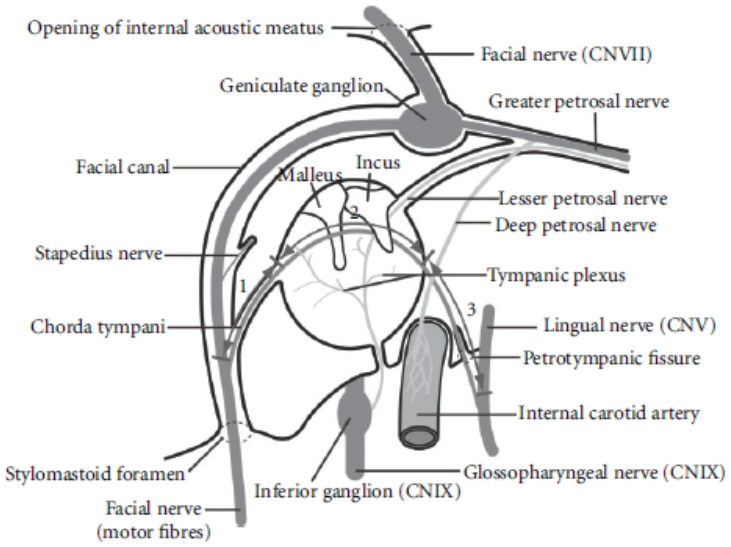

Figure 2.4: CTN portions between the facial nerve and the lingual nerve. Portion 1: mastoid process, portion 2: tympanic cavity, portion 3: submandibular fossa [14].

Inside the tympanic cavity, the chorda goes sideways with the stapes and crosses the ossicles between the malleus and the incus, on the medial surface of the neck of the malleus, as one can see in Figure 2.3. It then runs posteriorly and descending, close to the TM, and exits the tympanic box through the petrotympanic fissure. CTN provides parasympathetic innervation to submandibular and sublingual glands as well as special sensory taste fibers for the anterior two thirds of the tongue, through the lingual nerve [19, 20]. Besides being connected to taste sensation, this structure is also responsible for saliva secretion, as CTN is responsible for efferent innervation of the glands responsible for saliva production.

Some studies have been conducted along time in order to better understand the facial nerve and its branches, among which CTN, with several studies on diseases affecting such important nerves. Smith et al. studied FP as a consequence of facial nerve tumor [21]. They studied a case of a man with FP and taste loss in the right side of the face and tongue, that had a tumour behind the TM. This schwannoma was affecting the facial nerve, but the patient recovered well after surgery. The facial nerve is an extremely important nerve that is involved in facial expression, tears, taste and even hearing. Bell's palsy is a condition that can lead to facial nerve disorder. Other diseases, such as trauma, infection, tumours or genetic factors can also affect this nerve.

Several studies on the impact of CTN injuries on taste have been conducted. Most of these lesions were connected to taste aberrations and dry mouth. These symptoms are related to the main functions of this nerve, taste sensation transportation in the two anterior thirds of the tongue and facilitation of salivary production. Another of these studies was performed by Gopalan et al., that found that the stretch of CTN resulted in most significant symptoms of taste disturbance than CTN transection [22]. This kind of injuries is most of the times iatrogenic, meaning that they result from lesions during surgery. Michael and Raut (2007) reached the same conclusion, when they assessed operative findings on CTN [23]. Clark and O'Malley (2007) conducted an inves-

tigation including 42 patients that would undergo ear surgery, in order to study the influence of iatrogenic CTN injuries in taste sensation comparing cholesteatoma, a benign ear tumour, surgery with other middle ear surgeries [24]. Of all these patients, 21 had cholesteatoma, while the rest was having procedures as myringoplasty or stapedectomy to treat other ear condition. A total of 16 patients had their CTN completely sectioned, with only 5 (31%) showing symptoms of so. These symptomatic patients showed altered taste after surgery. However, symptoms had disappeared 6 months after. The same did not happen for myringoplasty and stapedectomy patientes that had CTN compressed or streched during the procedure, showing symptoms even 6 months after the intervention. Although in 5 of the 21 cholesteatoma cases CTN was slightly touched or stretched during surgery, none of these patients showed altered taste postoperatively. The results of this study support former research that states that taste disturbance can be quicker resolved when CTN is sectioned than in cases the nerve is compressed or stretched. The explanation may be that the conditions in which injuries due to surgery happen are different than those in which cholesteatoma affects this nerve, and so different outcomes will be observed when these lesions occur. This investigation also indicates that cholesteatoma leads to damages in CTN, as patients with cholesteatoma show less symptoms alteration after nerve injury during surgery, which indicates that the tumour leads to CTN hypofunctioning, as suggested in previous studies. This way, Clark and O'Malley findings also sustain the theory that symptoms are less intense and less frequent in patients that had chronic inflammation, once their nerves and ear structures were already working poorly. CTN recovery can be a slow process, taking up to 2 years. This way, a careful follow up must be done to fully assess its rehabilitation [25].

CTN was described in literature as having a diameter of between 0.3 and 0.5 mm, showing wide inter patient variation [26]. Nevertheless, there was a lack of information regarding CTN and its anatomy. Thus, some studies to better understand CTN position in the human head have been conducted. Trost et al. carried out a study to better assess the spatial relation of the CTN in the intratemporal fossa [27]. They considered that teaching CTN anatomy was a hard task due to the little spatial information there was about it. This way, CTN and other nerves were catheterized and X-ray and computed tomography (CT) scans examinations were carried out. The course of CTN was better studied and these findings contributed to raise the knowledge of head nerves. With the same goal in mind, and in order to better understand their spacial position to have better surgery outcome, Liu et al. studied the whole course of some deep nerves in human head [14]. Regarding CTN, dimensions showed wide inter patient variation. The obtained values for the part of the CTN that crosses the tympanic cavity were a diameter around 0.44 mm and a length of (9.83 ± 1.24) mm. The total length of CTN, from the facial to the lingual nerve, was about 54 mm. As already described in literature, CTN crosses the middle ear close to the ossicles and the TM, as shown in Figure 2.5. Literature states CTN arises from the facial nerve approximately 6 mm above the stylomastoid foramen. Nevertheless, the distance from CTN and the stylomastoid foramen was assessed by Liu et al., obtaining values from 5.93 to 21.63 mm, being the average 13.32 mm [14]. As there is no cover involving the CTN, this structure is highly vulnerable to the events that happen in its surroundings [28, 29].

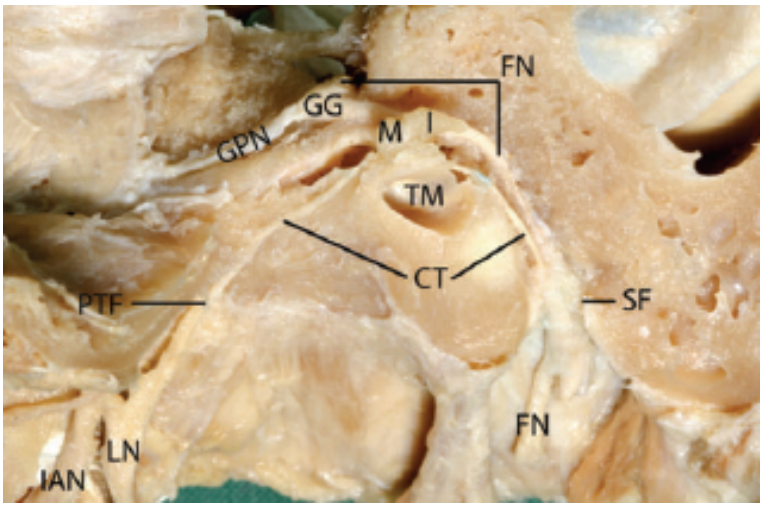

Figure 2.5: Dissection of the chorda tympani nerve from facial nerve, passing through the tympanic cavity and joining the lingual nerve. FN: facial nerve, I: incus, M: malleus, CT: chorda tympani nerve, GG: geniculate ganglion, GPN: greater petrosal nerve, CN: cochlear nerve, PTF: petrotympanic fissure, LN: lingual nerve, TM: tympanic membrane, SF: stylomastoid foramen, IAN: inferior alveolar nerve.

In 2015, a study was conducted to assess the degeneration of CTN, the major taste nerve, during COM [29]. As this structure runs uncovered in the middle ear, this investigation aimed to evaluate ultrastructural changes of CTN in different inflammatory middle ear diseases, namely simple COM and cholesteatoma. In order to do so, 10 CTN were analysed, 5 being controls and 5 being associated to COM or cholesteatoma, in which CTN was affected. The different data was analysed using electron microscopy. In the cases of unhealthy CTN, there were records of a higher portion of axon and myelin degeneration, which were associated to taste disturbance. Nevertheless, 3 of the 5 analysed damaged CTN showed signals of sprouting. This suggests that CTN has the ability to regenerate, which can justify taste recovery in the majority of cases.

2.1.3 Inner Ear

In the inner ear, the bone forms canals that are called bony labyrinth. This labyrinth is covered by connective tissue, periosteum, and in its inner part a similar but smaller structure is present, the membranous labyrinth. Two fluids fill the inner ear structures, endolymph and perilymph. The first fills the membranous labyrinth while the second fills the space between the bony and the membranous labyrinth.

The bony labyrinth is present in the main structures that belong to the inner ear, the cochlea and the vestibular system. While the first is directly connected with hearing, the latter, that comprises the semicircular canals and the vestibule, is involved in equilibrium function.

The stapes vibrations are transmitted to the inner ear through the round window. As the diameter of this structure is smaller than the one of the TM, when sound information travels from the middle to the inner ear, there is an amplification of the signal, important to overcome the impedance related to the cochlear fluid [30]. The round window is connected to the vestibule,

that communicates with the vestibular ramp, one of the cochlear chambers. The vestibular ramp goes from the oval window to the helicotrema, the peak of the cochlea. The tympanic ramp, other cochlear chamber, goes from the helicotrema to the round window, side by side with the vestibular ramp.

The portion of the cochlea next to the oval window is rigid and related to high frequency vibrations while the portion around the helicotrema is flexible and answers best to low frequency oscillations. Inside the cochlea it is possible to find the organ of Corti. It has more than thirteen thousand hair cells, that are very particular cells as they are able to transform pressure variations into electrical impulses.This way, it is possible to send the appropriate information to the brain, through the vestibulocochlear nerve.

2.2 Acoustics

Acoustic is the science field that dedicates to the study of sound. Sound can be described as a disturbance in the environment caused by a longitudinal mechanical wave, that makes the environment particles oscillate. This disturbance is caused by an emitter, that generates the sound, travels through the environment and reaches the receptor, the entity that receives the sound. Acoustic studies the phenomena involved in the generation, transmission and reception of sound waves. Since these are mechanical waves, they need a material so they can propagate, that can either be a solid, a liquid or a gas. When the emitter generates a sound, the particles around it oscillate, conveying the information to the surrounding particles. This movement goes on and on, making sound a pressure wave, meaning that there are compression areas, where there is a greater density of particles, and rarefaction areas, where one can find less particles. These areas alternate with each other along time, resulting in a sequence of compression and rarefaction, if one analyses a certain point for a period of time.

The main attributes of sound are pitch, intensity and timbre. Although sound is perceived differently by different people, the analysis of a sound is done with specific devices that quantify accurately the measured properties [6].

2.2.1 Frequency and Period

The frequency (f) is defined as the number of cycles during one second, being measured in cycles per second or Hertz (Hz) . On the other hand, the period (T) is the duration of a complete cycle, measured in seconds, in other words, it is the inverse of frequency, which is showed in Equation 2.1.

$$f = \frac{1}{T} \tag{2.1}$$

The human ear is capable of distinguish sounds with frequencies between 16 Hz and 20 kHz. Sounds which frequency is below 16 Hz are called infrasounds while the ones with frequency

higher than 20 kHz are ultrasounds. Frequencies up to 256 Hz are considered low, from 256 Hz to 1 kHz are considered medium, and above 1 kHz are considered high frequencies [6].

The way the ear grasps a sound frequency is called pitch. Thus, low frequencies are heard as low sounds whilst high frequencies are interpreted as high sounds, being this phenomenon connected to the area of the basilar membrane that suffers most excitation when a sound reaches the ear.

As mentioned before, sound waves are longitudinal mechanical waves. Wavelength (λ) is, by definition, the length a wave can travel in a period of time equal to T, and can be expressed through Equation 2.2, where C is the sound speed in the air and f is the wave frequency.

$$\lambda = \frac{C}{f} \tag{2.2}$$

This way, high sounds have low wavelength while low sounds have high wavelength.

2.2.2 Intensity and Pressure

Sound intensity is connected to the amplitude of a sound wave. It is defined as the sound power, in watts, per unit of area and its unit is W/m^2. Sound intensity level (L_I) establishes the relation between sound intensity (I) and an intensity reference value (I_o), equal to 10^{-12} W/m^2, through the expression presented in Equation 2.3 [31].

$$L_I = 10 \times log(\frac{I}{I_0}) \tag{2.3}$$

Sound pressure is related to the pressure oscillation suffered in a certain point due to a sound wave. As mentioned before, sound waves are pressure waves. That being said, when a sound wave reaches a certain point, the pressure in that point, that was previously the atmospheric pressure, will suffer an alteration, increasing and decreasing its value.

Sound pressure level (SPL) relates pressure variations with a reference pressure value. The decibel is used, as the ear reacts with a logarithmic behaviour and so, a logarithmic expression is easier to address. The SPL decibel scale establishes a sound level by comparing sound pressure (p) with a reference pressure value (p_0), equal to 2×10^{-5} Pa, that indicates the audibility threshold. Equation 2.4 establishes this relation.

$$SPL = 20 \times log(\frac{p}{p_0}) \tag{2.4}$$

The human ear can detect sounds between 0 and 120 dB SPL, which correspond to 20 μPa and 20 Pa if one is referring to pressure [32].

2.2.3 Timbre

Timbre is the sound attribute that allows to distinguish sounds with the same intensity and pitch coming from different sources. It is an intricate sound characteristic hard to quantify.

2.2.4 Impedance

The acoustic system present in humans can be interpreted as an electrical circuit, where the fluid movement is the electric current and the pressure variation is the equivalent tension in that part of the circuit. This way, the impedance (Z) of a fluid through an area can be obtained through the quotient of the pressure exerted in that area (p) and the volumetric speed (U), expressed in Equation 2.5.

$$Z = \frac{p}{U} \tag{2.5}$$

Specific acoustic impedance (z) can be obtained through the quotient between pressure (p) and speed of a certain environment (v), as shown in Equation 2.6. This physical quantity can be useful for calculations where transmission between environments happens.

$$z = \frac{p}{v} \tag{2.6}$$

2.3 Middle Ear Diseases

Hearing loss is considered to have a significant impact on the Global Burden of Disease, states the World Health Organization (WHO). This happens mainly in industrialized countries [33].

Different conditions may be associated with the auditory system. According to their location and severity, they will present different repercussions to one's health. Although deafness can happen due to a genetic condition or pregnancy complication, hearing loss may occur, among others, by virtue of virus, bacteria or trauma [1].

Great intensity sounds may be responsible for ear damage. Environments with long lasting high intensity sounds like concerts or certain jobs are, therefore, nefarious for people's hearing health. These kinds of sounds can lead to structural and functional alterations in the ear structures.

Hearing damage may result in deafness, which can be total or partial, permanent or temporary. Deafness can be associated to problems with sound transmission, due to damage in the external or middle ear. However, it may also be connected to injuries in the most inner part of the auditory system and so related to sensorineural hearing loss.

Some ear disorders can also be responsible for hearing loss. As the part of the ear under study in the current work is the middle ear, some diseases associated to this part of the ear are briefly described.

Middle ear diseases can be caused by virus, bacteria or some other ear diseases, such as tympanosclerosis or otosclerosis. OM includes acute OM (AOM) and COM, with and without effusion [1]. It consists in an infection and consequent inflammation in the middle ear. It can start due to the Eustachian tube blocking and its malfunction hinders the otitis treatment. Most of the times, it can be treated through antibiotics.

Myringosclerosis is a hyalin or sclerotic modification, a change in the hardness properties of the mucous membrane of the TM that results from an accumulation of calcium phosphate [34]. If

it does not reach an advanced stage of development, it can be treated through a tympanoplasty. If this condition proceeds, spreading to the ossicles, it becomes a tympanosclerosis [35, 36]. This condition is characterized by an intense fibroblast activity, which leads to collagen deposition. Tympanomastoidectomy is normally the surgery that can treat this disease.

Otosclerosis is a disorder of the stapes that influences the fixation of this ossicle. This disease is characterized by an absorption of bone by osteoclasts and consequently substitution with a denser and harder bone, which results in stapes footplate fixation, leading to stapes immobilization [37]. This phenomenon will be an obstacle to sound propagation in the middle ear, causing conductive hearing loss, as the sound will have trouble in propagation. This disease can lead to a hearing loss between 0 and 50 dB [38]. Stapedectomy, a surgery in which this bone is replaced by a prosthesis, is the typical solution.

Ossicular chain discontinuity can also happen [2]. A separation of the middle ear ossicles can occur after a chronic infection in the ear, as it can deteriorate parts of the ossicles, or as a consequence of a trauma. In the majority of the cases, the problems occur in the joint between the incus and the stapes. This discontinuity will lead to hearing loss as sound information will have to struggle hard to proceed to the inner ear.

TM perforation is another injury that can lead to hearing loss or even vertigo. It consists of a hole in the TM and it makes the middle ear susceptible to infection. It may need surgery to be treated. The reason behind a TM perforation may be a middle ear infection, unbalanced external ear and middle ear air pressure or even a loud sudden sound.

In the following subsection, OM and its consequences will be further discussed.

2.3.1 Otitis Media

OM is one of the most common childhood infections and the one responsible for the majority of children's hospital visits, antibiotics consumption and surgeries in developed countries [39, 40]. In the US, it is estimated that 3 to 5 billion dollars are spent yearly in OM related expenses. However, in reality this amount should be higher, once indirect costs may be underestimated [41]. It is estimated that almost every children will experience at least one OM episode during its childhood [1].

As mentioned before, this condition may manifest in different ways, as an acute disease or as a chronic one.

AOM is children's major cause of morbidity, being a middle ear infection characterized by an intense acute pain and, sometimes, escorted by fluid in the middle ear, which is called OM with effusion [39]. Studies show that, on average, until the age of three, children will experience one episode of AOM each year [1]. Despite being much more frequent in children, AOM incidence is decreasing for all ages [42]. AOM incidence was determined in 2005. Records show an incidence between 45% and 60% for children under five years old, between 19% and 22% for children from

[2] Ossicular descontinuity. https://ent.keckmedicine.org/condition/ossicular-chain-discontinuity/ Accessed on 29-01-2020

five to fourteen, 3.1% to 3.5% from fifteen to twenty four years old and between 1.5% and 2.3% for adults aged 25 and older [43].

When the infection proceeds for more than 3 months, it is considered a COM. Usually, this condition is associated with a TM perforation unable to heal or to an OM without recovering. While AOM appears much more commonly in young children, COM and problems derived from it are more frequent in older children and adults [44]. According to WHO, COM has a prevalence of around 1% in general population in developed countries [45].

COM can present itself as a simple COM or cholesteatomatous COM. Simple COM can be non-infected or with effusion. The first is caracterized by the existence of a hole in the TM with no fluid accumulation in the middle ear. People are able to live with this condition for an indefinite period, as far as the ear stays dry. Surgery to repair the hole may be needed as prevention or to improve hearing. COM with effusion is characterized by the existence of fluid inside the middle ear, due to an infection. The fluid can be serous, mucous or even pus [30]. The standard treatment for this type of COM is antibiotics. A concerning possibility is the cholesteatomatous COM. In this case, there is the development of a cholesteatoma, a benign pouch like lesion formed by skin cells and exfoliated keratin debris in the middle ear [3]. Cholesteatoma development can happen either if the TM is perforated or if the Eustachian tube is blocked despite the TM not being perforated. This can happen due to Eustachian tube malfunction, since this way a good ventilation of the middle ear does not happen, hampering the otitis treatment. In addiction, Eustachian tube malfunctioning may also lead to partial vacuum in the middle ear, that can pull the TM inwards, creating a cyst that can develop to a cholesteatoma, as showed in Figure 2.6.

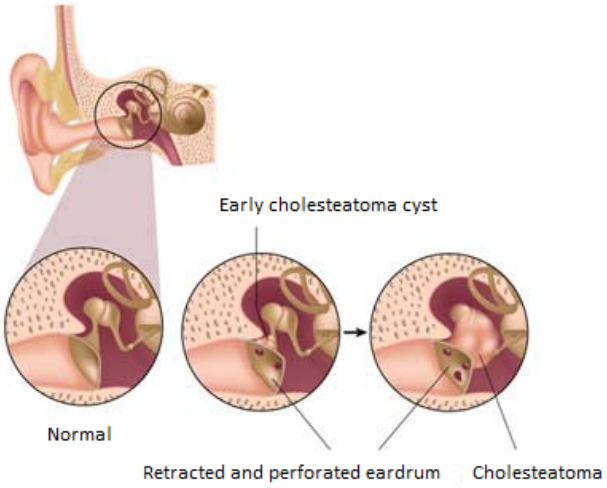

Figure 2.6: Example of cholesteatoma development due to Eustachian tube malfunction [3].

COM may be the source of severe complications. If the infection is capable of spreading itself outside the middle ear, it can lead to critical situations. If the infection is able to make its way to the mastoid bone, a mastoiditis can occur. It can also disseminate to the inner ear, leading to an infection that may cause dizziness. If it arrives to the brain, it can origin meningitis or even

brain abscess. Although these complications are uncommon, COM surveillance is of the utmost importance.

In order to assess ossicular chain degradation and discontinuity caused by COM, Haidar et al. conducted a study including 279 ears that underwent surgery due to COM [46]. A part of the patients had cholesteatoma. In their study, they found that the ossicular chain showed erosion in 23,66% of the analysed patients. It was also found that erosion is correlated with cholesteatoma, as 69,3% of the patients with this disease had their ossicular chain eroded. The incus was, of the three ossicles, the most affected by osteoclastic activity. It is then necessary to be alert to this condition as this phenomenon may highly compromise hearing.

2.3.1.1 Cholesteatoma

A cold can lead to the Eustachian tube blocking. If this happens, infection due to fluid accumulation in the middle ear may happen, as the ear ventilation is not proper and so it becomes harder to treat the otitis, that can develop to a more critical condition, as it is a cholesteatoma.

A cholesteatoma is a keratinized squamous epithelium that can grow within the middle ear. It is a benign tumor, that can either be congenital - due to genetic factors, embryologic phenomenon or pregnancy complications - or, in the majority of the cases, acquired [47].

It is estimated that cholesteatoma has an incidence of 9.2 per 100 000 habitants a year in northern Europe countries [48]. Thus, considering that a primary care practitioner sees around 2 500 patients in its working life, he is expected to have one new cholesteatoma case each four to five years [48]. The incidence of cholesteatoma is higher in children from 5 to 15 yearls old, being the average age for acquired cholesteatoma diagnosis 9.7 years. Men are more likely to develop acquired cholesteatoma, being the ratio men/women for acquired cholesteatoma around 1.4 [47].

Despite being benign lesions, cholesteatomas should not be ignored as they are connected to infections and hearing loss. The development of a cholesteatoma will possibly lead to the erosion of the nearby structures due to its expanding nature and surrounding inflammatory reaction [3]. This inflammatory reaction will release several molecules, namely lytic enzymes, cytokines and growth factors, that can recruit osteoclasts, capable of destroying bone cells [47]. This can result in permanent damage in the middle ear ossicles, culminating in severe and conductive hearing loss, once the ossicle chain can even be interrupted due to ossicle degradation. Moreover, a cholesteatoma that grows attached to the ossicles will also contribute to damping phenomena, leading to hearing loss, as there will be an extra mass that will affect sound transmission through the ossicles. Furthermore, tumour properties evolve along time, making the tumour a harder and denser structure as it grows. This way, the larger the tumour, the more sound damping.

The WHO conducted a study on global costs of unaddressed hearing loss, in 2017, also assessing the cost-effectiveness of preventive measures and interventions [49]. Unaddressed hearing loss results in significant costs to the health-care system. This way, WHO considers that hearing

[3]Cholesteatoma, Author: Dr. Harrison Lin https://harrisonlinmd.com/conditions/cholesteatoma/ Accessed on: 2020-01-29

loss must be considered a public health matter. With this in mind, public health measures for prevention and early diagnosis of hearing loss would be cost-effective. Hearing loss implies several costs. Direct costs are normally the ones incurred by health-care systems and also the costs of special support for deaf people adaptation. Indirect costs comprise the incapacity of individuals to contribute to the economy. In addiction, there is also the stigma experienced by patients that suffer from hearing loss, as well as the problems associated with the loss of all the experiences that involve sound. Costs associated with adaptation of children with moderately severe hearing loss to educational environment and support for communication also have to be considered. The global cost associated with unaddressed hearing loss in the world is estimated as 750 to 790 billion dollars. Despite being a value challenging to obtain, informal care and intangible costs, namely social exclusion, may increase this value in about 104 billion dollars, in a global scale [49]. Thus, prevention and early diagnosis of ear diseases such as cholesteatoma would be helpful to reduce these costs.

COM together with a cholesteatoma may lead to damages in CTN, the facial nerve branch that crosses the middle ear. Considering that nerves are fragile structures, if a middle ear cholesteatoma grows near the CTN, it can affect this nerve. The CTN may be pressured and stretched or it can even be torn due to cholesteatoma growth. According to the lesions caused by this mass, CTN may be able to recover its functions when pressure fades away or, in more concerning cases, lesions in the nerve may be permanent, which can possibly result in FP.

The connection between CTN and cholesteatoma development in its surrounding was studied by Hu and Wang (2001), who carried out a research of the CTN related to the appearance of a cholesteatoma [50]. In their study, 19 cholesteatoma cases were studied in terms of taste and facial nerve functioning. CTN damages have been registered in all cases, namely swelling and disarrangement. Two patients suffered from taste alteration after surgery and FP has not occured in any patient. The study conclusions suggested that cholesteatoma leads to ultrastructural changes of the CTN.

Cholesteatoma development in the middle ear is still an intriguing process in some aspects. The origin and growth pattern of a cholesteatoma has been a matter of study for a long time. In 1873, Wendt [51] suggested that a cholesteatoma could develop due to squamous metaplasia fissure in the middle ear. Later on, Palva et al. (1968) [52] and Sade et al. (1982) [53] indicated that squamous epithelium of the middle ear mucosa could be the source of acquired cholesteatoma. Wells and Michaels (1991) studied four temporal bones of patients with cholesteatoma, proposing that an acquired cholesteatoma resulted from TM retraction pockets due to Eustachian tube malfunction. They also concluded that inflammation is an important factor for the growth of cholesteatoma [54]. Nowadays, there are several reasonable theories for the origin of cholesteatomas, being the latter one of the most acceptable.

The link between FP and OM and cholesteatoma was also a matter of interest. With this in mind, Takahashi et al. (1985) conducted a study to assess this connection. In the hospital from which the data was obtained, 1 638 patients were examined due to problems of FP. From all these cases, only 50 people also showed presence of OM, which corresponds to 3.1% [55]. Although

some of these patients showed AOM, the majority was experiencing COM, as there were 17 cases of COM with effusion and 22 cases of COM with cholesteatoma. These investigators concluded that only 2% to 4% of the FP cases occurred due to OM. They also concluded that FP caused by COM usually occurred together with cholesteatoma or acute increase of inflammation in the middle ear, being the paralysis mild and its progression slow. This research group also considers that a FP that results from a COM must be treated through surgery. They state the tympanic portion of the facial nerve is the most susceptible to inflammation as its cover is very thin in this segment. Savic and Djeric (1989) conducted a study including 1 261 patients that were subjected to a surgery due to COM. Of all these patients, 64 showed FP before surgical intervention, 42 (66%) of them being considered complete paralysis and 22 (34%) of them incomplete. When looking for a cholesteatoma presence, they found it in 52 (80%) of these patients. According to this data, one can see that FP is highly connected to cholesteatoma following COM. After surgery, complete recovery was managed in 45 (70%) of the patients, partial recovery in 15 (24%) and failure happened in 4 (6%) of the patients that suffered from FP [56]. That being said, surgery can be considered an efficient approach to restore facial function after incomplete or complete paralysis. Also with the aim of studying FP caused by COM and understanding the effects of a cholesteatoma and surgery outcome, Yetiser et al. (2002) conducted a research with 24 patients with FP [57]. During surgery, doctors found cholesteatoma in 17 patients (70.8%). The latter and other 3 patients with no evidence of tumour also showed bone destruction. After the intervention, 14 patients (58.3%) showed recovery within 3 months. This way, it was concluded that FP caused by COM appears most of the times as a consequence of a cholesteatoma.

It was also found that if a cholesteatoma is positioned in the anterior epitympanum or in the petrous apex there is an increased danger of FP. Peron and Schuknecht reported some cases of petrous apex cholesteatoma where a fifth of the patients showed FP. Atlas et al. discovered nerve dysfunction in 7 of the 14 studied cases where a petrous apex cholesteatoma was present [28].

Former studies show that there is a close connection between pressure and the induction of osteoclastic bone resorption that is typically associated to cholesteatomas. Thus, Orisek and Chole conducted a research on the pressure exerted by cholesteatomas on nearby structures [58]. This way, they used pressure gauges to measure the static pressure employed by the tumours. The results pointed to pressures between 1.31 mm Hg and 11.88 mm Hg being the ones that lead to greater osteoclastic activity. Another important aspect was the size of a cholesteatoma. This way, cholesteatomas were also studied in terms of dimension and proportion in the middle ear [3]. Their maximum length in transverse and coronal planes was measured, through magnetic resonance imaging (MRI). In this study, 164 ears were analysed, being 102 (62%) male and 62 (38%) female, with ages from 6 to 77 years old. The values for cholesteatoma diameter obtained in this research fluctuate between 4 and 27 mm, being the median value 9 mm. As scarce information was found regarding reference values for the pressure exerted by a cholesteatoma as well as their size, these two studies were the ones considered in the current work.

Some of the cholesteatoma's symptoms may include a sense of pressure in the ear, headache and fluid drainage. Swelling, redness and pain behind the ear can also happen. In more concern-

ing cases, hearing loss, vertigo and FP are also possible to be experienced by patients with this condition [4].

As cholesteatomas may occur as a consequence of a simple COM, these symptoms may, at the beginning, be mistaken as a simple OM. In other cases, this mass can also appear as a silent condition, with no significant symptoms in the beginning. However, as it develops, symptoms should start to intensify.

A cholesteatoma can present a diagnostic challenge. Although it can be diagnosed in an early stage, as it can be associated with a COM that may be surveilled by a doctor, it can also develop with no clear symptoms nor cause.

Cholesteatomas can be identified during a visit to the doctor, through ear examination and symptoms analysis. Using specific devices, doctors can properly analyse the ear behaviour. An otoscope, that allows to look into the ear, can be used for examination. With this device, doctors can look for the presence of a cholesteatoma, searching aggregations of skin cells or a large mass of blood vessels in the ear.

Through devices that allow obtaining high quality images and procedures that provide information on the ear functioning, doctors can perform accurate diagnosis.

An audiometry is a test that can determine patients hearing levels as well as their acoustic reflex and ability to discriminate between different sound intensities. The results are useful to diagnose hearing loss. Approaches like audiometry may help to diagnose the extent of a lesion.

CT and MRI are also important techniques that enable a careful assessment. These are imaging procedures, that allow to obtain 2D slices of the analysed structures. The first uses several X-ray measurements captured from different angles combined using computational processes. The second makes use of strong magnetic fields, not involving X-rays or other ionizing radiation. CT of the temporal bone without contrast is a widely used diagnostic imaging technique within the otolaryngology field. MRI can also be helpful in diagnosis. These techniques are of major significance for surgery planning and provide doctors with essential information on the area of interest [47]. This is extremely important as surgery is the main treatment option in case of cholesteatoma [59].

Although antibiotics treatment may be enough for a simple COM, the infection might remain, leading to the appearance and development of a cholesteatoma. In this case, the situation asks for a surgery to remove the infected tissue and repair the TM perforation and other lesions that may have occurred in the ear during the tumour growth. This is a delicate procedure due to the affected structures dimensions. Tympanomastoidectomy is, usually, the selected surgery for cholesteatoma removal. Two main different approaches can be chosen, canal wall up or canal wall down, being the main difference that, in the latter, the posterior part of the ear canal is removed. This way, the most frequently used of these procedures is canal wall up, while canal wall down mastoidectomy is more commonly used when the cholesteatoma is already in an advanced stage [3, 47]. Tumor

[4] Cholesteatoma Ear Cysts: Symptoms, Diagnosis, Treatment https://www.webmd.com/cold-and-flu/ear-infection/benign-ear-cyst Accessed on: 2020-01-30

resection is usually performed by the time the patient visits the doctor showing symptoms, which differs from patient to patient.

Hearing ability may or may not be fully recovered after surgery as cholesteatomas are able to recruit osteoclasts, which may lead to the erosion of the ossicles in such a way that the chain is interrupted, leading to conductive hearing loss.

Patients that suffer from FP due to the pressure exerted by a cholesteatoma usually recover the facial functions after cholesteatoma removal, as the pressure on the nerve vanishes. The time period for this recovery can go up to some months. However, if for some reason the cholesteatoma causes irreparable damages in the nerve, facial function may never return to normal.

After surgery, it is important to do a careful follow-up as the cholesteatoma may reappear. Usually, a second surgery is planned 6 to 18 months after the cholesteatoma removal, in order to assess if there is any chance of recurrence or if any residues were left behind. Alternatives to surgery, as MRI and some otoscopic and auditory exams, become more frequent, in order to avoid surgical intervention. This is extremely useful as surgical intervention for the first cholesteatoma removal may deform the ear anatomy, in case a canal wall down is performed. If a canal wall up technique is used, the cholesteatoma may reappear in difficult areas to access and inspect, usually requiring a second-look surgery. New MRI techniques arise, namely diffusion-weighted MRI, that provides image contrast in regard to the capability of water molecules to diffuse through tissues [60]. This reliable approach was proven to be efficient as a substitute for a second-look procedure in former studies, as besides avoiding surgery, it does not comprise any risks from radiation exposure. Diffusion-weighted MRI is considered sensitive as well as specific for recurrent or residual cholesteatoma detection.

The most critical period when referring to cholesteatoma recurrence are the first two years after surgery, as the majority of reported cases happens during this term [3].Recurrence of 26.9% was obtained in a study conducted by Syms and Luxford in 2003 [61].

2.4 Biomechanical models of the ear

A technological approach for medical problems is to develop models of the part of the human body that one wants to study in detail and use them to assess the desired conditions. Previously developed computational models have been used to study the ear. Some of these projects are mentioned in this section. Furthermore, some projects that led to the current biomechanical ear model that was used in this thesis are presented.

With the purpose of better studying the auditory system, several computational models of the ear have been developed over time. This is of major importance and a benefit to students as these models enable them to better understand the intricate anatomy of the ear and to better relate the two dimensional structures present in the literature to the real three dimensional shapes and positions. Some of these projects are briefly described below.

Wang et al. (2006) created a three dimensional virtual model of the temporal bone to promote a better knowledge of this bone's anatomy among science and, specifically, medicine students

[62]. The model included the temporal bone itself, cochlea - endolymph and perilymph spaces as well as the sensory epithelia of both cochlear and vestibular labyrinths, the middle ear ossicles and muscles, the TM, the carotid artery and the vestibular, cochlear and facial nerves. The structures transparency could be controlled and the model could be sliced in any section. This model is available for download.

Gan et al. (2006) developed a model of the ear based on 780 histological sections of 20 μm thickness obtained from a temporal bone [63]. The 3D model included the middle ear cavity, ossicles and ligaments as well as air in the tympanic cavity and external auditory canal. FEM was used to discretize these structures. The impact of different frequencies was analysed in this model, studying the pressure distribution in the middle ear. The results were assessed by measuring the effects of sound in the oval and round windows as well as in the umbo. The influence of TM perforation was also studied using this model. This model is presented in Figure 2.7.

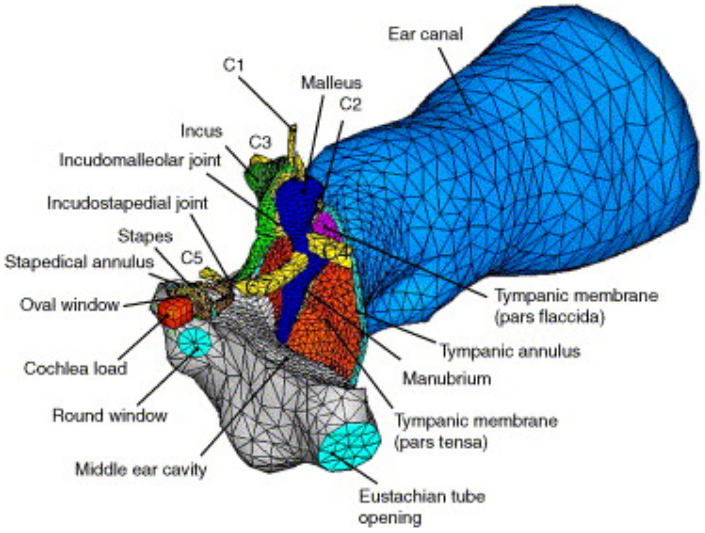

Figure 2.7: Ear model developed by Gan et al. (2006) [63].

An year later, Gan and a different group of researchers conducted another investigation of the ear, this time including also the cochlea (comprising basilar membrane, vestibular scale and tympanic scale) and its fluids [64]. The group obtained the middle ear transfer function, which includes the TM movements, as well as the stapes footplate's and round window's. Sound pressure gain in the middle ear was also measured. The addiction of the cochlea was important so cochlear impedance could also be studied. The obtained values matched the ones reported in literature. Furthermore, the cochlea model made it possible to associate sound stimulus in the external ear with basilar membrane vibration, proving the good functioning of this part of the model.

Lui et al. (2009) developed a model of the ear that included the auditory canal, TM, middle ear ossicles, suspension ligaments and muscles, and middle ear cavity and inner ear fluids, once again using FEM [65]. Some ear disorders were studied, namely malleus handle defect, hypoplasia of incus long process and the defect of stapes crus, in order to better understand their consequences in

sound transmission. The results were compared to the ones in literature, leading to the conclusion that the developed model was capable of predicting ear mechanisms.

With the aim of better assessing implantable hearing devices, Zhang and Gan (2011) developed a finite element model of the ear that included the ear canal, TM, middle ear ossicles and ligaments and cochlea, based on histological sections of a temporal bone [66]. The analysis included acoustic phenomena, ear structure and fluid coupling in the ear. The main goal of their work was to understand middle ear and cochlear implants functioning and the better way of implantation. The middle ear transfer function was obtained through this project. Zhang and Gan model can be seen in Figure 2.8.

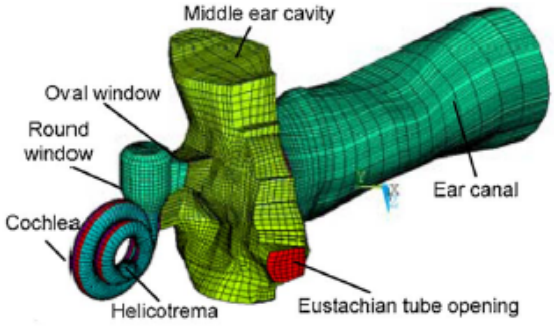

Figure 2.8: Ear model developed by Zhang and Gan (2011) [66].

"The visible ear" is one of the most relevant computational models of the ear, since it allowed, for the first time, a high-fidelity study of the temporal bone anatomy as well as accurate middle ear surgery training. The major goal of this work was to obtain a high resolution digital model of the temporal bone. Before this project, the existing image libraries were created by independent researchers and the access was restricted due to copyright protection and poor image quality. A fresh frozen human temporal bone was used as a model, being collected 605 CT images that were used to create the model. The image quality was improved and size variation corrected. In the end, this project provided high quality images that could be used as source material for human ear model development [67]. In 2007, Wang et al. developed a three dimensional virtual model of the ear, using the images provided by the project “The visible ear” [68]. This 3D model allows to fully rotate the structures, control visibility and transparency and even slice the model at any desired section, being available for whoever wants to work with it. Several projects that used this model have been carried out by the research group that proposed the current work, in order to better understand the middle ear structures behaviour under certain conditions. Thus, many contributions to the model have been done during the last years. Some examples of such projects are described below.

Gentil (2008) conducted a study on the ear using, firstly, a model based on middle ear structures dimensions and geometry, described by Anson e Donaldson [69], and then based on imaging exams. A model of the ear including TM, ossicles, joints, ligaments and muscles as well as cochlear impedance was developed. Static and dynamic studies were conducted for a frequency

band between 100 and 10 000 Hz for different levels of sound pressure, between 0 and 120 dB, applied in the TM. Umbo and footplate displacements were obtained and analysed. In this work, ligaments were given hyper-elastic behaviour. This was the first project including muscular contact and activation as well as considering footplate rotations.

Garbe et al. (2010) studied the rehabilitation of the middle ear, analysing the orientation of the TM intermediate layer as well as the pressure values registered in the tympanic box. In addiction, the umbo and footplate displacements for different sound intensities applied in the TM were also studied [30].

Areias et al. (2014) developed a biomechanical study of two middle ear pathologies, OM and otosclerosis. Two slightly different models were studied, a simpler one and a more complex one. The first comprised TM, middle ear ossicles, ligaments and tendons, cochlear fluid and part of the temporal bone. The complex model included all the mentioned structures plus air in the external auditory canal and tympanic cavity, skin, jaw and ear cartilage. The study showed that, under OM condition, a decrease in umbo and footplate displacements could be observed. This happened for all frequencies in the case of the umbo and mostly for frequencies around 1kHz for the footplate [7].

The effect of TM perforations and myringosclerosis in the mechanical behaviour of the middle ear ossicles and in the TM was studied by Gentil et al. (2014), using FEM. It was concluded that for micro perforations no disparities are observed. For a 7 mm perforation, the displacement of the ossicular chain suffers a reduction, which is connected to hearing loss [70].

In 2016, Areias et al. carried out a study to better describe sound transmission in the human ear [71]. Thus, and based in the project "The visible ear", they developed a three dimensional model of the ear, using FEM. Once again, two biomechanical models were used, a simple and a complex one, being the difference that the latter also considered air in the external ear canal and tympanic cavity, including as well the cartilage, jaw and skin. The magnitude and phase angle of the umbo and stapes footplate displacement were obtained. Figure 2.9 shows the mentioned models.

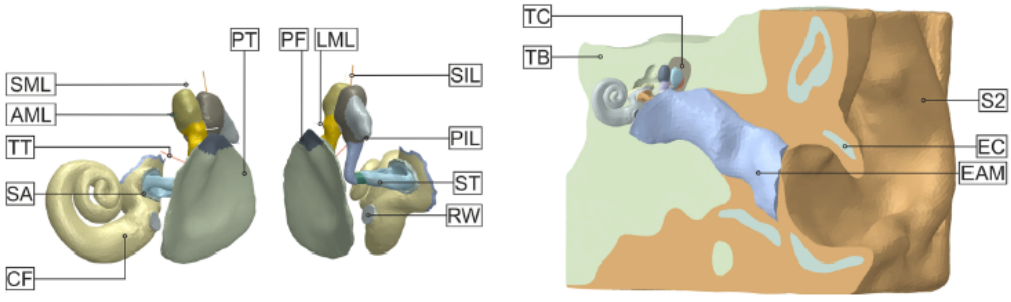

Figure 2.9: Ear Model developed by Areias et al. in 2016 [71]. Simpler model without temporal bone (left) and complex model sectioned (right). SML - superior mallear ligament, AML - anterior mallear ligament, TT - tensor tympani tendon, SA - stapedius annular ligament, CF - cochlea, PT - Pars Tensa, PF - Pars Flaccida, LML - lateral mallear ligament, SIL - superior incudal ligament, PIL - posterior incudal ligament, ST - stapedius tendon, RW - Round Window TC - tympanic cavity, TB - temporal bone, S2 - skin, EC - ear cartilage, EAM - external auditory meatus.

With the purpose of analysing the consequences of OM with effusion on sound transmission, Areias et al. (2017) conducted another investigation, using the same computational model, with the necessary adjustments to the desired analysis [72]. The results obtained in this study allowed to calculate the magnitude and phase in both the umbo and the stapes normalized velocities, which made it possible to describe how the presence of fluid in the middle ear cavity influences hearing. It was proven that fluid in the middle ears leads to a decrease in the response of the normalized umbo and stapes velocity.

Savaris et al. (2018) studied the influence of different sized irregular bodies attached to middle ear structures, namely incus, stapes and TM. These bodies intended to mimic tumours. The only tumour that affected hearing was the one connected to the TM, that was also the bigger one [4].

In the current work, the same ear model will be used. In Figure 2.10 the middle ear structures as well as their medial and lateral neighbours present in the existing model are represented. Through this image, it is possible to understand which middle ear structures were already present and would surround the tumours that would be studied in this project as well as the CTN structure, that would be developed and analysed in the present dissertation.

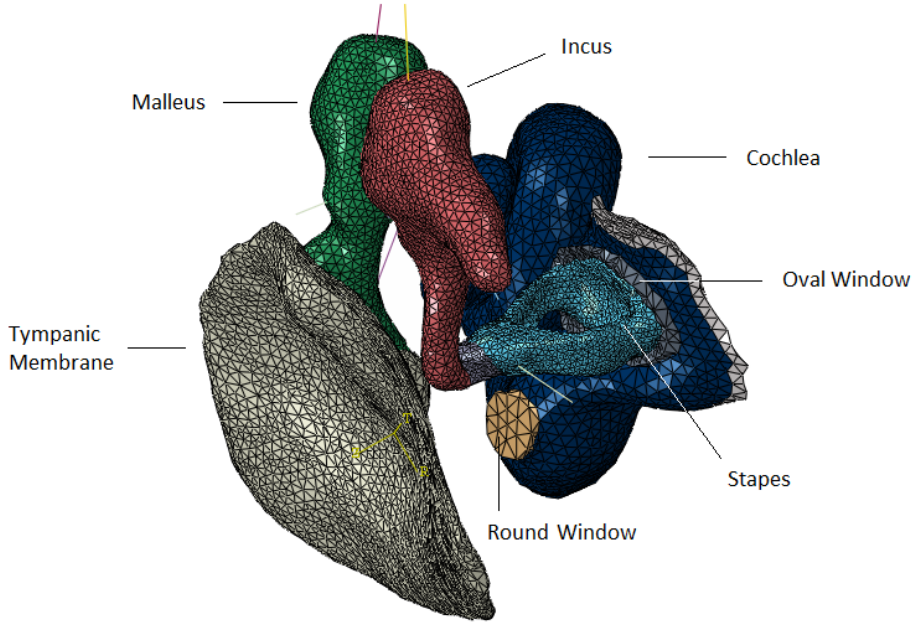

Figure 2.10: Current Ear Model.

There has been considerable improvement in computational models over time. Reliable techniques to automatically detect and segment human structures through medical exams have risen, which also contributed to better modeling. This way, and together with a better knowledge of the ear properties and functioning, better ear models are being developed along time.

Overall, despite having some limitations in what concerns to accurately mimic the human body functions, computational models bring a lot of advantages in the medical field as they allow to simulate and study diseases and phenomena that would be extremely difficult to analyse otherwise.

Chapter 3

Methodology

During the development of this dissertation, an existing computational model of the ear was enhanced, since a new structure, the CTN, was added. In addiction, the behaviour of the ear in the presence of different sized cholesteatomas, which were also modeled, was assessed.

Biological structures are very complex to analyse due to their irregular shapes. In order to conduct a biomechanical study of such structures, some helpful methods have been developed. One of the major obstacles consisted of the difficulty in analysing these structures as single continuous structures.

To surpass the obstacle of analysing continuous bodies, the FEM arises. This method is a numeric approach that allows a close mathematical approximation to complex differential equations. This way, to solve a problem that includes a continuous domain using FEM, the domain is split into several parts, named elements, obtaining a mathematical description for their behavior. This process is called discretization, resulting in a set of finite elements, each of them corresponding to a finite portion of the continuous domain. The vertices of the elements are called nodes. This way, it becomes much easier to solve a complex problem. FEM was used to develop the biomechanical study of the presence of a cholesteatoma in the middle ear.

It is important to mention that, to solve these problems, computational methods are in most cases required, due to the complexity of the calculus. There are many simulation softwares that make use of FEM. The present work was developed using Femap and ABAQUS softwares, being the first used to model the different structures and the latter to run the desired simulations [73].

3.1 Ear model

As previously mentioned, a model of the ear had already been developed and it was used during this work. This model was based in the project "The visible ear" of Sorensen et al. [67]. This project main goals were to develop a temporal bone atlas as well as a computational model that allowed for virtual simulations in the middle ear, in order to better study this structure and even surgery planning. Using Abaqus software [73], the different parts of the ear model were discretized and properly connected.

The model characteristics are described below. The middle ear is usually described as a linear system when analysing sound transmission from the TM to the cochlea [74]. Thus, elastic behaviour materials were considered for the different structures. Poisson's coefficient was considered 0.3 for all the model parts. The assigned Young's modulus for the different structures are present in the following tables. Regarding damping, $\alpha = 0s^{-1}$ and $\beta = 0.0001s$ were the chosen values for all entities.

The dimensions of the structures that were modeled in previous works were compared with literature values obtained by Wever and Lawrence (1982), being both the model and the reference values for each structure presented below [10].

The bone part is the cover of all the ear structures present in the model. Figure 3.1 shows the finite element mesh of the bone. In Table 3.1 some mesh informations are shown and in Table 3.2 the mechanical properties assigned to the bone are presented. The mentioned element type, C3D4, corresponds to three dimensional tetrahedral elements with 4 nodes.

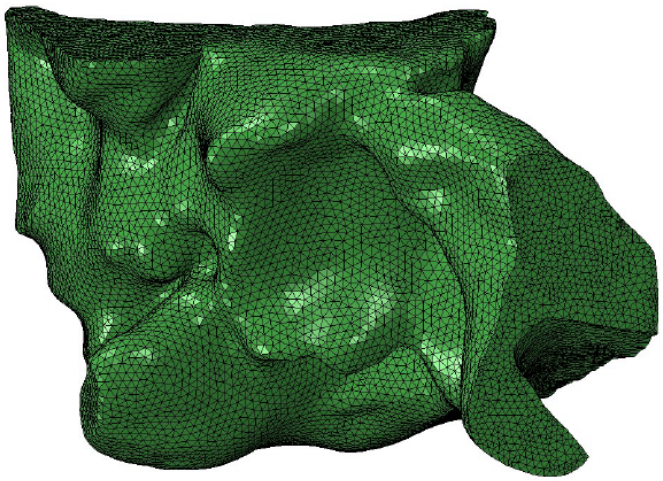

Figure 3.1: Finite element mesh of the bone.

Table 3.1: Bone mesh information.

	Elements	***Nodes***
Number	499891	96634
Type	C3D4	-

Table 3.2: Mechanical properties of the bone.

	Properties
Density (kg/m^3)	2.0×10^3
Young's Modulus (N/m^2)	1.41×10^{10}

The finite elements mesh of the TM can be seen in Figure 3.2. This image shows TM *pars flaccida* and *pars tensa*. Table 3.3 shows the dimensions of the modeled TM and the correspondent literature values [10].

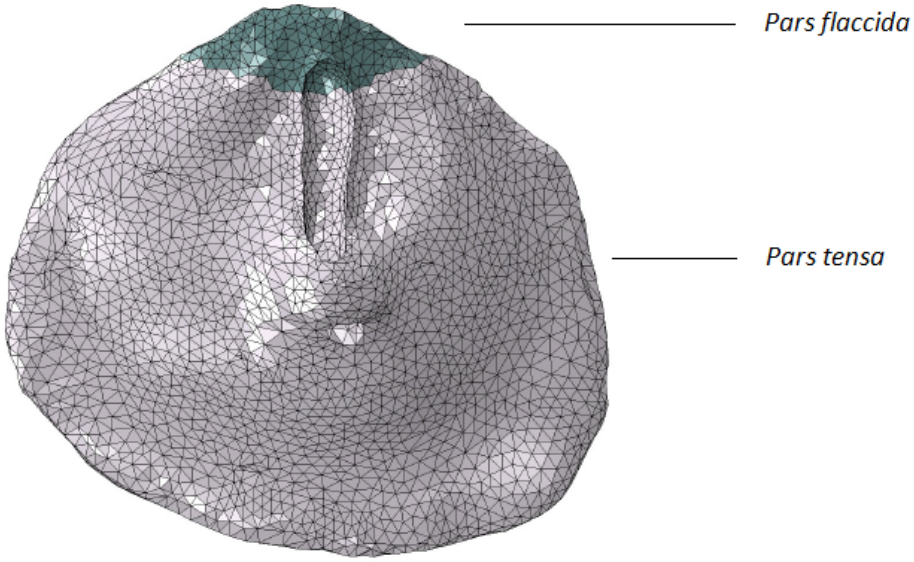

Figure 3.2: Finite element mesh of the tympanic membrane.

Table 3.3: Dimensions of the modeled TM and correspondent literature values [10].

	Parallel to the manubrium length (mm)	***Perpendicular to the manubrium length (mm)***	***Thickness (mm)***
Model	9.45	10.22	0.2 - 0.5
Literature	8.0 - 10.0	7.5 - 9.0	0.1

Both the perpendicular to the manubrium distance as well as the TM thickness are a bit higher than expected, being this difference bigger for the thickness. Nevertheless, as the structures geometry was obtained through a highly precise technique, the model values were accepted. The information regarding the finite element mesh are described in Table 3.4 and the considered mechanical properties for the TM, considering that it is an orthotropic structure, are described in Table 3.5. The tympanic sulcus was simulated by using a low Young's modulus, 6×10^3 N/m^2. This part is composed by 1 916 elements (C3D4).

Table 3.4: TM mesh information.

	Elements (Total)	***Elements Pars Tensa***	***Elements Pars Flaccida***	***Nodes***
Number	19495	18542	953	5455
Type	C3D4	C3D4	C3D4	-

Table 3.5: Mechanical properties of the TM.

Properties	***Pars Tensa***	***Pars Flaccida***
Density (kg/m^3)	1.2×10^3	1.2×10^3
Young's Modulus (N/m^2) (radial)	3.2×10^7	1.0×10^7
Young's Modulus (N/m^2) (circunferencial)	2.0×10^7	1.0×10^7

Figure 3.3 shows the finite element mesh of the malleus as well as its different parts, head, neck and manubrium. Table 3.6 shows the model and literature values for the malleus. Although this ossicle dimensions are reasonable given the reference values, the model mass is too high. Through Table 3.7 it is possible to know the informations related to the malleus mesh. The mechanical properties of the material associated with this ossicle are present in Table 3.8.

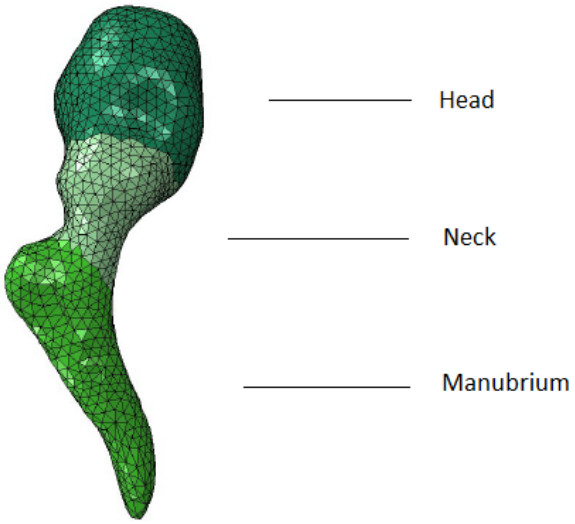

Figure 3.3: Finite element mesh of the malleus.

Table 3.6: Dimensions of the modeled malleus and correspondent literature values [10].

	Total length (mm)	***Manubrium length (mm)***	***Mass (mg)***
Model	8.55	4.89	48
Literature	7.6 - 9.1	5.8	23 - 27

Table 3.7: Malleus mesh information.

	Elements (Total)	***Elements Head***	***Elements Neck***	***Elements Manubrium***	***Nodes***
Number	16222	8111	3722	4389	3485
Type	C3D4	C3D4	C3D4	C3D4	-

Table 3.8: Mechanical properties of the malleus.

Properties	***Head***	***Neck***	***Manubrium***
Density (kg/m^3)	2.55×10^3	4.53×10^3	3.70×10^3
Young's Modulus (N/m^2)	1.41×10^{10}	1.41×10^{10}	1.41×10^{10}

In Figure 3.4, the finite element mesh of the incus and its different parts, body and short, long and lenticular apophysis, are shown. Table 3.9 allows to compare the obtained values for the model with reference values [10]. Although one can see the incus model mass is higher than the expected, the dimensions are really close to the values published in literature by Wever and Lawrence. Through Table 3.10 it is possible to know the informations related to the mesh of the incus. The defined mechanical properties of the incus material are expressed in Table 3.11.

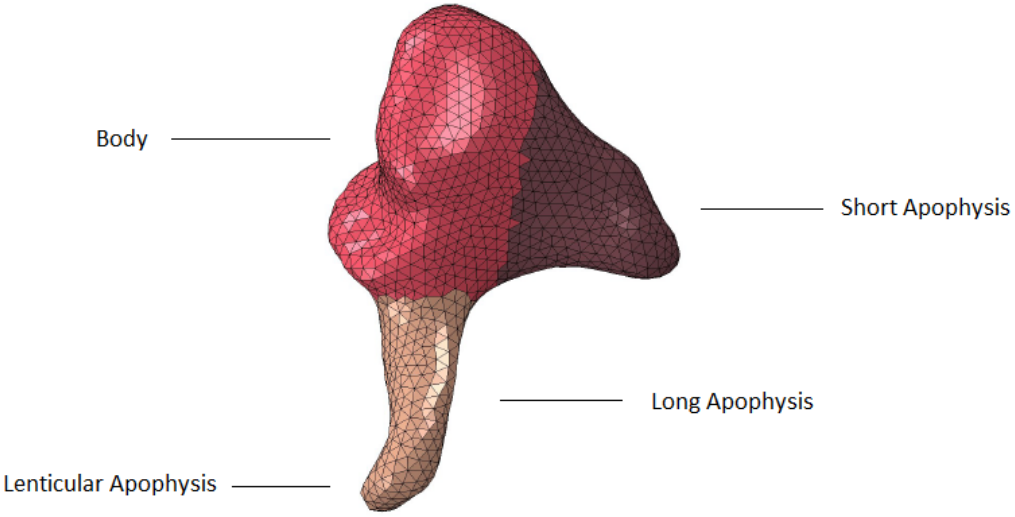

Figure 3.4: Finite element mesh of the incus.

Table 3.9: Dimensions of the modeled incus and correspondent literature values [10].

	Parallel to short apophysis length (mm)	***Parallel to long apophysis length (mm)***	***Mass (mg)***
Model	4.95	7.26	47.7
Literature	5.0	7.0	25 - 32

Table 3.10: Incus mesh information.

	Elements (Total)	***Elements Body***	***Elements Short Apophysis***	***Elements Long Apophysis***	***Nodes***
Number	18749	11874	4261	2614	3966
Type	C3D4	C3D4	C3D4	C3D4	-

Table 3.11: Characteristics of the incus.

Properties	***Body***	***Short Apophysis***	***Long Apophysis***
Density (kg/m^3)	2.36×10^3	2.26×10^3	5.08×10^3
Young's Modulus (N/m^2)	1.41×10^{10}	1.41×10^{10}	1.41×10^{10}

Figure 3.5 shows the finite element mesh of the stapes. In Table 3.12, the stapes dimensions as well as the values stated in literature can be compared [10]. The modeled stapes mass is higher than the reference values. Table 3.13 gathers the mesh information regarding this ossicle and in Table 3.14 stapes properties are shown.

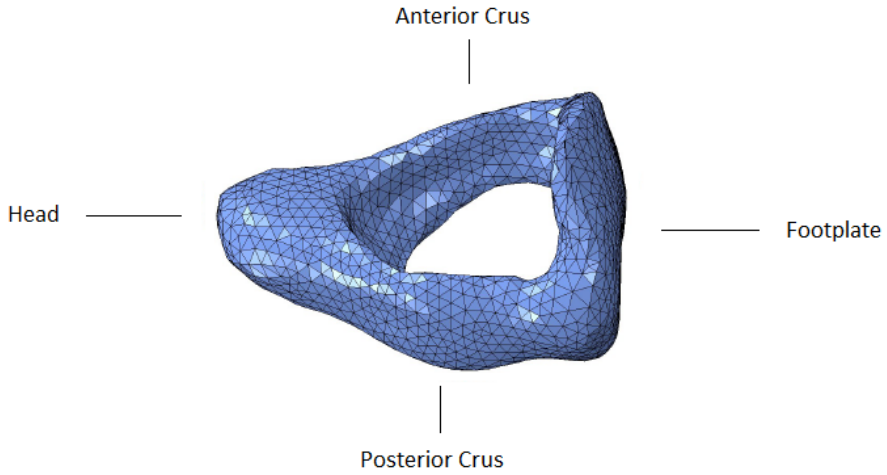

Figure 3.5: Finite element mesh of the stapes.

Table 3.12: Dimensions of the modeled stapes and correspondent literature values [10].

	Footplate to the top of the head length (mm)	***Footplate length (mm)***	***Footplate width (mm)***	***Mass (mg)***
Model	3.82	3.09	1.92	10.2
Literature	2.5 - 4.0	2.64 - 3.36	0.7 - 1.66	2.05 - 4.35

Table 3.13: Stapes mesh information.

	Elements	***Nodes***
Number	17692	3995
Type	C3D4	-

Table 3.14: Properties of the stapes.

	Properties
Density (kg/m^3)	2.20×10^3
Young's Modulus (N/m^2)	1.41×10^{10}

The TM, ossicles, ossicle joints, ligaments and muscles are represented together in Figure 3.6. Elements and nodes information for both the incudomalleolar and incudostapedial joints are described in Table 3.15. The joints were considered to show an elastic behaviour, being their properties described in Table 3.16.

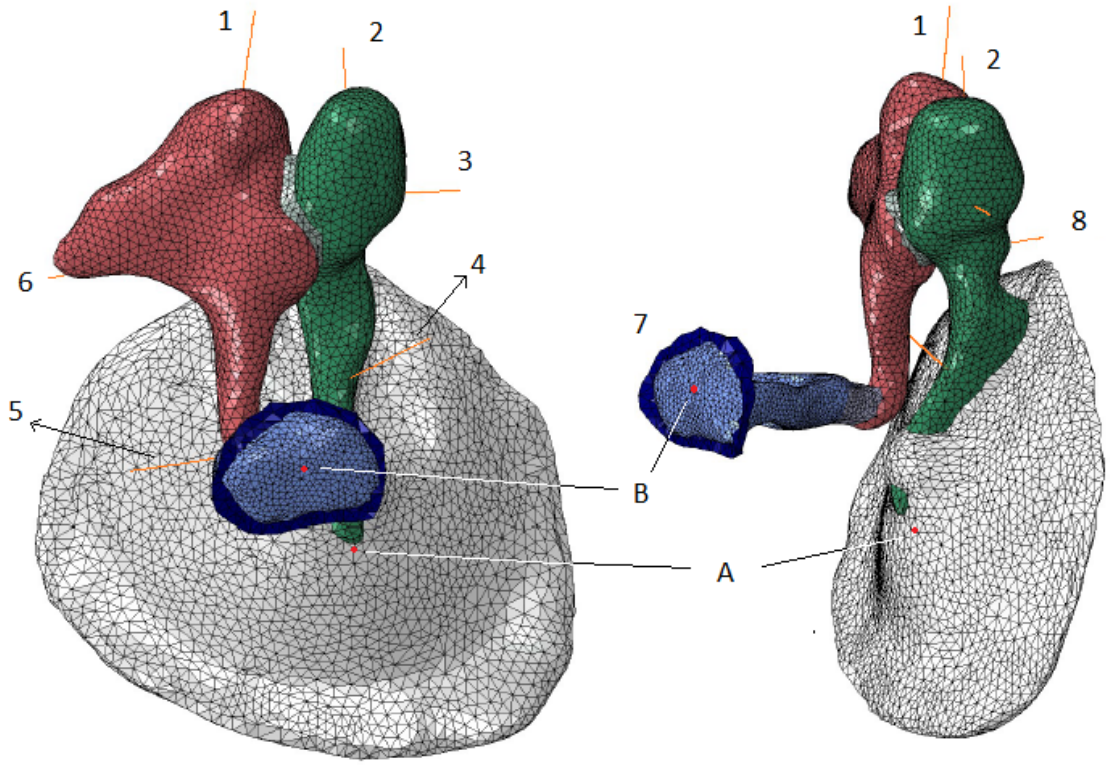

Figure 3.6: Finite element mesh of the middle ear structures. 1 - Superior malleal ligament, 2 - Superior incudal ligament, 3 - Anterior malleal ligament, 4 - Tensor tympani muscle, 5 - Stapedial muscle, 6 - Posterior incudal ligament, 7 - Annular ligament, 8 - Lateral malleal ligament, A - analysis node in the umbo, B - analysis node in the stapes footplate.

Table 3.15: Ossicles joints mesh information.

	Incudomalleolar joint		***Incudostapedial joint***	
	Elements	***Nodes***	***Elements***	***Nodes***
Number	988	336	1057	320
Type	C3D4	-	C3D4	-

Table 3.16: Ossicle joints properties.

Joints	***incudomalleolar***	***incudostapedial***
Density (kg/m^3)	3.2×10^3	1.2×10^3
Young's Modulus (N/m^2)	1.41×10^{10}	6.0×10^5

The behaviour of ligaments and muscles was also assumed as elastic, being the properties in Tables 3.17 and 3.18. The ligaments and muscles were represented through T3D2 elements, being the first beam elements and the latter linear. The annular ligament was made with 641 elements (C3D4) and 314 nodes, that connect it with the stapes.

Table 3.17: Ligaments properties.

Ligaments	***Superior Malleus***	***Anterior Malleus***	***Lateral Malleus***	***Superior Incus***	***Posterior Incus***	***Annular Stapes***
Young's Modulus (N/m^2)	4.9×10^4	2.1×10^6	6.7×10^4	4.9×10^4	6.5×10^5	1.0×10^4

Table 3.18: Muscles properties.

Muscles	***Tensor Tympani***	***Stapedius***
Young's Modulus (N/m^2)	2.6×10^5	5.2×10^5

The appropriate boundary conditions were then applied. In the TM, the tympanic sulcus allows for the connection with the bone. This was simulated by fixating the borders of the TM. Inside the tympanic cavity, the malleus, the incus and the stapes are connected to each other through the joints. In addiction, they are hold by ligaments and muscles, which was simulated by connecting these structures to the corresponding ossicle, in one end, and fixate it in the other, in order to mimic its connection to the tympanic cavity wall. Finally, the anular ligament connects the stapes to the bone, so it was also fixated. The bone was encastered in the extremities.

In the work of Areias, a dynamic analysis was performed, in order to obtain the natural frequencies of the model as well as the umbo and footplate displacements for frequencies between 100 Hz and 10 kHz, for several sound pressure values [7]. Initially, this pressure was applied in the TM, and, on a second stage, in the outer part of the air inside the external ear canal. For this work in particular, the same analysis was performed, being the pressure applied directly in the TM. The studied sound pressure levels were 60 and 80 dB SPL, as these are intermediate values and the results would be analogous for other values. The displacements were assessed in the same locations as the previous project, the umbo, in the TM, and the centre of the stapes footplate. These locations are evidenced in Figure 3.6, through letters A and B, respectively.

3.2 Cholesteatomas

In order to simulate a tumor growth, three different sized tumours were built. The chosen area for the tumours was the connection between the malleus and the incus, as the development of a tumour in this location would affect CTN, which was one of the topics of investigation in this thesis. The main goal was to assess the effects of these masses on both hearing and possible facial paralysis. The cholesteatomas were built with an ellipsoid shape, considering that the bigger one should be large enough to get close to the CTN so it was possible to test the effect of the tumor squeezing the nerve against the incus.

According to Lips et al., a cholesteatoma diameter in the three axes oscillates between 4 and 27 mm [3]. With this in mind, the three tumors were built. Their dimensions can be seen in Table 3.19 and their meshes information in Table 3.20.

Table 3.19: Dimensions of the three modeled tumours.

	Diameter 1 (mm)	***Diameter 2 (mm)***	***Diameter 3 (mm)***
Small tumour	3.97	2.73	1.86
Medium tumour	4.90	3.26	2.86
Large tumour	5.80	3.50	3.15

Table 3.20: Mesh information of the three modeled tumours.

	Small tumour		***Medium tumour***		***Large tumour***	
	Elements	***Nodes***	***Elements***	***Nodes***	***Elements***	***Nodes***
Number	6556	1044	13003	2101	17669	2859
Type	C3D4	-	C3D4	-	C3D4	-

The smaller tumor was the first to be created. Regarding the dimensions mentioned in the table, three diameters were measured, along three different axes. Diameter 1 concerns the vertical measurement, diameter 2 is measured in a perpendicular axis, being connected to the distance along the incudomalleolar joint, from the malleus to the incus, diameter 3 is in the same plan that diameter 2, but perpendicular to it, measuring the depth of the tumor. It is possible to see that this tumour dimensions are reduced, when comparing them to literature values. As this tumour is still in its initial stage of development, it would not be likely to trigger any symptoms. This way, the fact that these values are not among the ones described in literature is acceptable. The cholesteatoma and its position in the middle ear are shown in Figure 3.7. The three axes are also evidenced in this image.

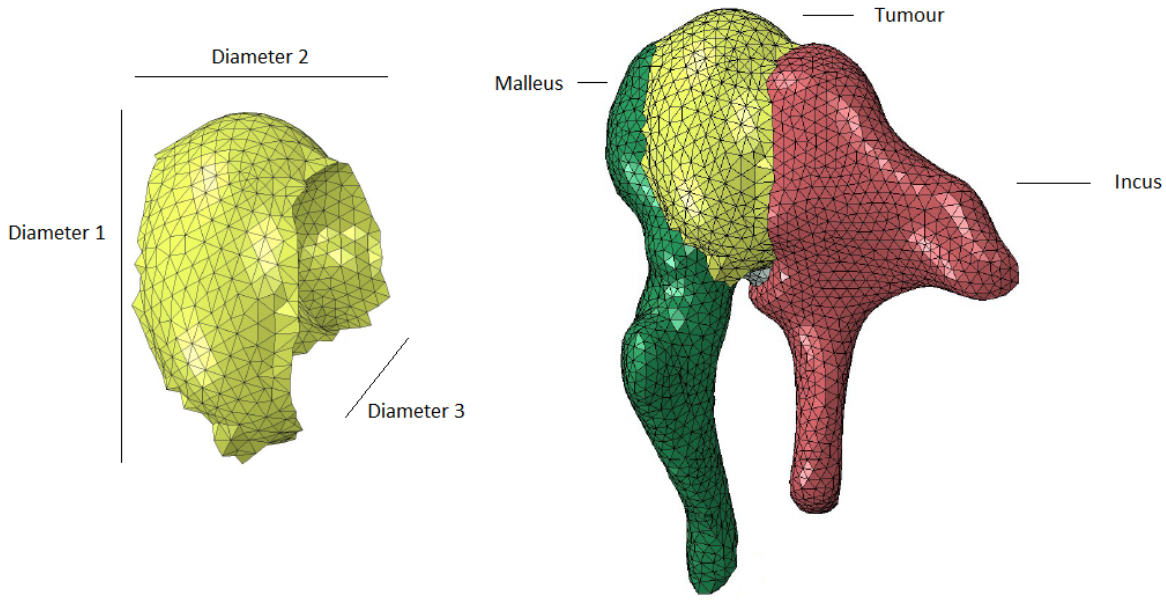

Figure 3.7: Small tumor finite element mesh. Left - small tumour, right - small tumour in its position in the ossicular chain

Next, the medium tumour was created. It was bigger than the first one, but not big enough to reach the CTN. Diameters 2 and 3 are, once again, slightly lower than reference values, as one can see in table 3.19. Figure 3.8 shows the tumour and its position in the ossicular chain.

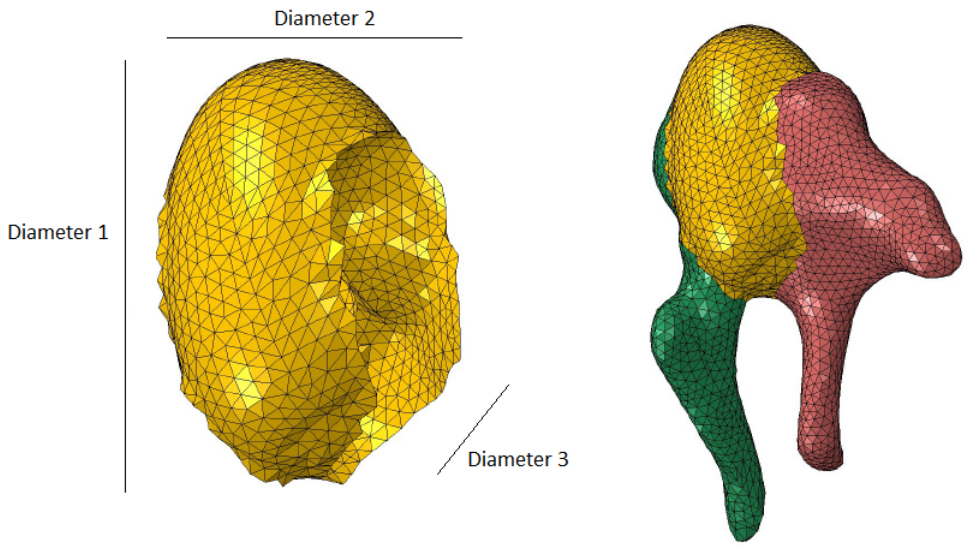

Figure 3.8: Medium tumor mesh. Left - medium tumour, right - medium tumour in its position in the ossicular chain.

Finally, the third tumour was created. This was the larger one. This tumour dimensions are closer to the acceptable values described in literature. Figure 3.9 shows the tumour and its position in the ossicular chain. The larger tumour was designed considering that it should be able to reach CTN and squeeze it against the incus.

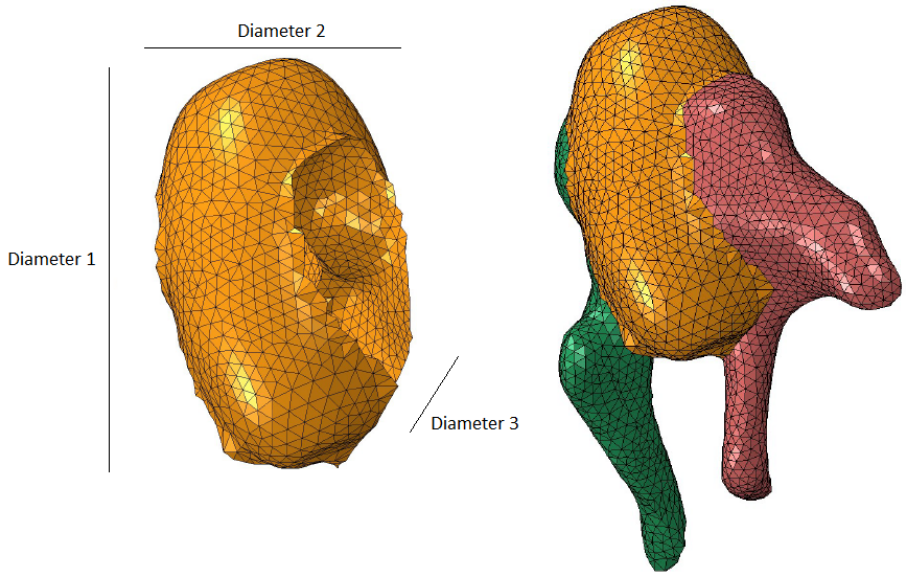

Figure 3.9: Large tumor finite element mesh. Left - big tumour, right - big tumour in its position in the ossicular chain.

Initially, the three tumours were considered to have similar properties. According to Raveh Tilleman et al., that studied cancerous tissue mechanical properties, this tissue Poisson's ratio is 0.43 ± 0.12 and the Young's modulus is, on average, 52 kPa [75]. This way, an elastic behaviour considering these values was defined for the created cholesteatomas. The density of the tumours was assumed as $1.2 \times 10^3 kg/m^3$.

To create the tumours, their geometry was constructed and the surface mesh was generated. This mesh was then attached to the ossicles, with some of the tumours elements using malleus and incus nodes. After this, the tumours volume was filled with tetrahedral elements with 4 nodes (C3D4).

Figure 3.10 shows the different tumours created so the tumour growth was simulated.

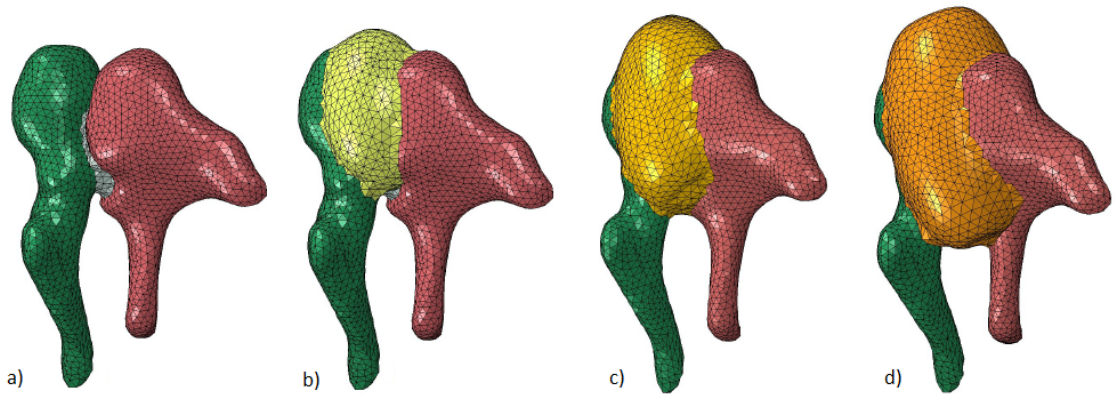

Figure 3.10: Simulation of tumour growth. a) healthy state (no tumor), b) small tumour, c) medium tumour, d) large tumour.

Once the tumours and their finite elements meshes were created and their properties defined, this data was added to the already existing model and new results were obtained. The same dynamic analysis as in the work of Areias was conducted for the simple model with the three different sized tumours [7]. The studied sound pressure levels were 60 and 80 dB SPL.

The displacement of the footplate was analysed for the healthy case, with no tumor, and for the three different tumor sizes. The chosen nodes for this analysis were nodes A and B, represented in Figure 3.6, as these are a node in the umbo and a central node of the stapes footplate, respectively.

After these first simulations, and as cholesteatomas' properties vary along their development, becoming harder and denser structures, new simulations were performed for the larger tumour. This time, the chosen properties were similar to the ones of the ossicles, being its Young's modulus $1.41 \times 10^{10}\ N/m^2$, its Poisson's coefficient 0.3 and its density $2.36 \times 10^{-9}\ kg/m^3$, equal to the incus body. The simulations were conducted for the same frequencies and pressures as before.

Finally, a simulation considering that cholesteatomas cause the degradation of the nearby structures was performed. As mentioned before, cholesteatomas are able to recruit osteoclasts, that lead to bone destruction. With this in mind, and in order to mimic this phenomenon, the properties of the parts of the ossicles wrapped by the tumour were modified to be equal to the tumours'. This simulation intended to mimic the replacement of the ossicles by the cholesteatoma in the regions that were degraded by the osteoclasts. This way, these elements were manually selected and their properties were modified, for the three tumour sizes. Once again, the simulations were performed for the same frequency band and SPL values.

The phase angle of the displacement of the footplate and the umbo was also analysed for the four cases, healthy and three tumour sizes, as well as for the larger tumour with properties similar to the ossicles and the case in which degradation was considered, for the large tumour.

3.3 Chorda Tympani Nerve

Considering that one of the main goals was to model the CTN, and in order to improve the existing ear model, CTN was also modeled in the course of this dissertation. This structure was developed and built from scratch and incorporated in the computational model. Although there was scarce literature regarding this structure dimensions, possibly because it is such a tiny structure, the gathered content on this topic was organized and exposed in Chapter 2. This allowed to properly establish the structure's path inside the tympanic cavity, the portion of interest of CTN for the current work. In order to do so, it was important to know the exact dimensions and particularities of this nerve.

As stated by Liu et al., the mean value obtained for the diameter of the CTN's section that crosses the middle ear is 0.44 mm [14]. The CTN length measured inside the tympanic cavity was (9.83 ± 1.24) mm [14]. According to these values and supported by the description of the nerve course, in Section 2.1.2.1, it was possible to create a reliable computational representation of the CTN. Adding Figures 2.4, 2.5 and 3.11 to the previous information, it was then possible to define CTN geometry and finally build a finite element model of the CTN, as seen in Figure 3.12.

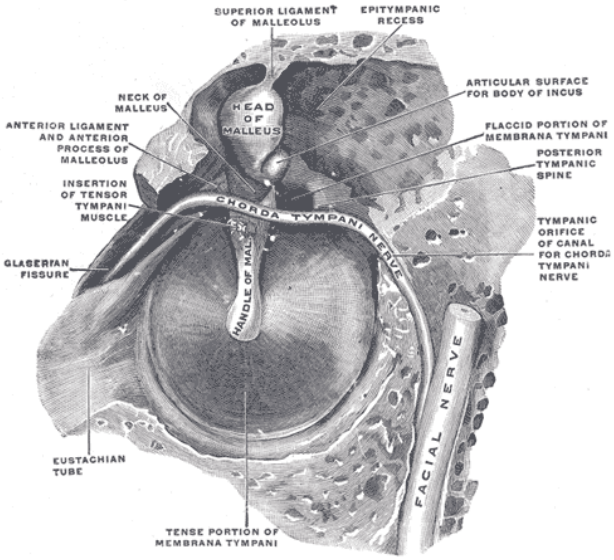

Figure 3.11: CTN position and course in the middle ear [76].

Figure 3.12: Finite element mesh of the CTN, medial view.

The diameter and length of the created CTN as well as the literature values are presented in Table 3.21. Comparing these values, it is possible to see that the modeled structure has a superior length than what would be expected. Nevertheless, these values have high interpatient variation and there are measurements records of the tympanic portion of CTN close to the created structure length, present in Appendix A.1.

Table 3.21: CTN dimensions and correspondent literature values [14].

	Diameter (mm)	***Length (mm)***
Model	0.44	13.3
Literature	0.44	8.59 - 11.07

The mesh details are listed in Table 3.22 and the defined properties for the CTN are present in Table 3.23. Due to scarce information regarding CTN properties, these values were based on a study regarding the mechanical properties of the sciatic nerve, conducted by Liu et al. [77].

Table 3.22: CTN mesh information.

	Elements	***Nodes***
Number	2052	2875
Type	C3D8	-

Table 3.23: CTN characteristics.

	Properties
Poisson's Coefficient	0.37
Young's Modulus (N/m^2)	4.1×10^7

Figure 3.13 shows CTN in its position in the middle ear. In Appendix B.1 it is possible to see the middle ear model before and after the CTN assembly, from three different perspectives.

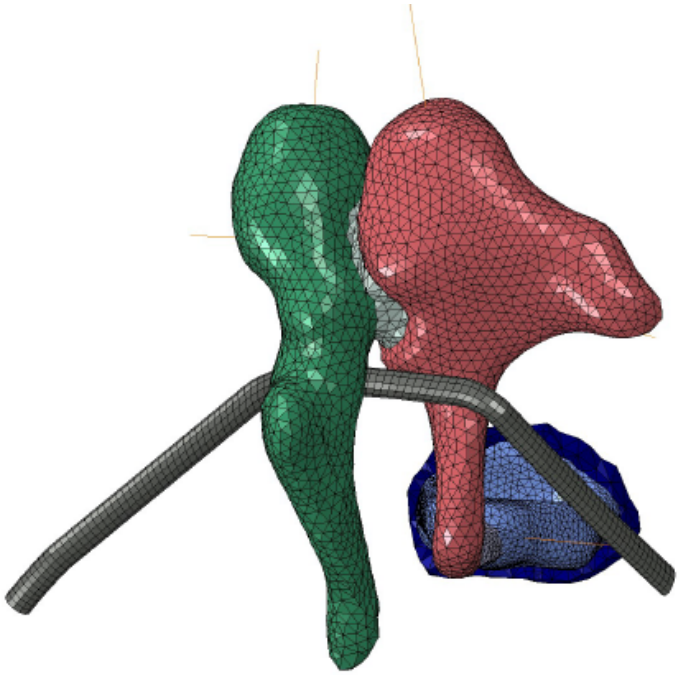

Figure 3.13: CTN in the middle ear, lateral view.

After modeling and meshing CTN in the appropriate position, this structure was properly adjusted to the ossicles so their meshes articulated perfectly with no overlapping. After this, the simulations were performed. The main goal was to understand the behaviour of the CTN when pressured by a cholesteatoma. This way, and as described in the previous section, three different sized tumours were created. The small tumour could not reach the CTN, the medium one was able to establish the first interaction with CTN and only the bigger tumour was large enough to wrap the CTN and pressure it against the ossicles. The simulations were performed considering that the CTN would be initially pushed down and then, with the tumour growth, pushed against the incus.

The first simulations were made using the medium tumour, as a way to simulate the first interaction between the CTN and the cholesteatoma. As the idea was to simulate the pressure exerted by the cholesteatoma growth, an internal pressure was defined to simulate it. Thus, a shell with the tumour shape was created and connected to the ossicles. As previously mentioned, Orisek and Chole reported the pressure exerted by a cholesteatoma as between 1.31 mmHg (approximately 174 Pa) and 11.88 mm Hg (approximately 1 584 Pa). Thus, as this tumour is still in an intermediate state of development, a pressure of 174 Pa was applied in the internal surface of the shell. Figure 3.14 shows the spatial relation between CTN and the medium tumour. The CTN was fixed in its extremities and the ossicles were totally immobilized. The part of the shell connected to the ossicles was also fixed. The tensions were analysed in three different nodes of the CTN, as showed in Figure 3.14. The chosen nodes were C, a central node in the part of the CTN that is pushed down in the first interaction between the CTN and the cholesteatoma, D, a central node in the part of CTN that contacts with the incus, the ossicle against which the CTN would be pressed, on the side on which the cholesteatoma will apply pressure, and E, not visible in the representation, a central node in the part of the CTN that would be pressed against the incus, in the opposite side of node D.

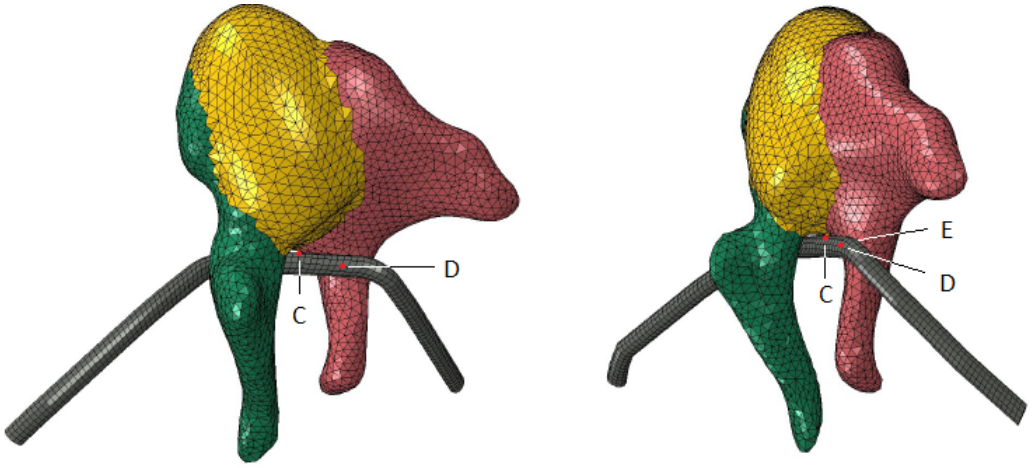

Figure 3.14: CTN and medium tumour in the middle ear. C, D and E are nodes in which the results of applying pressure on CTN were assessed.

Then, the interaction between the CTN and the large tumour was studied. In order to do so, the tumour had to be adjusted to the CTN, as the initially created large tumour was occupying some of the area that belongs to the CTN. After the adjustment, the same procedure described above for the medium tumour was followed. Figure 3.15 shows the spatial relation between CTN and the large tumour. Instead of applying an internal pressure of 174 Pa, a higher value between the pressure interval described in the work of Orisek and Chole (174 - 1 584 Pa) was used. As it is a large tumour, but it can still grow and be capable of exerting higher pressures on the surrounding structures, the chosen value for this simulation was 1 300 Pa. The results were analysed in the same nodes.

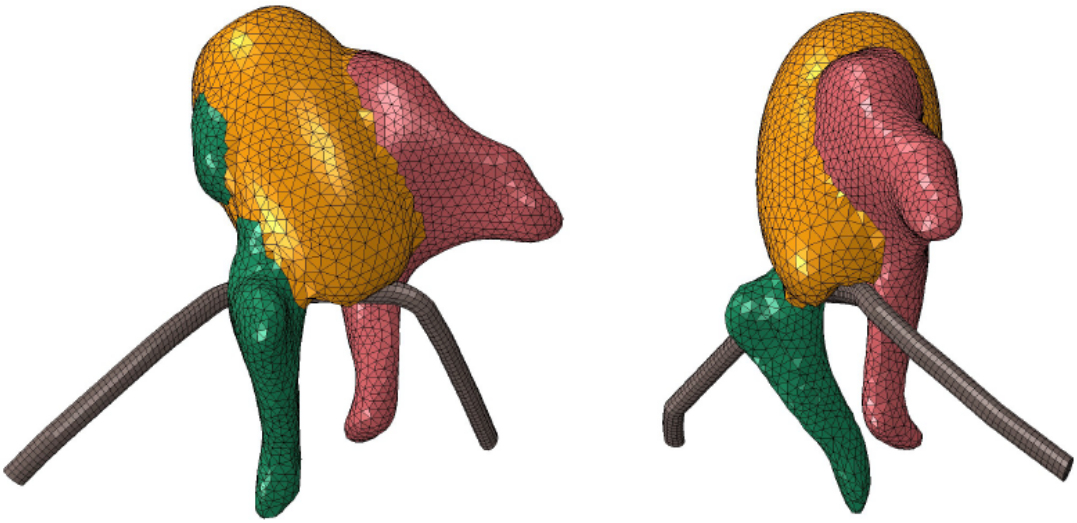

Figure 3.15: CTN and large tumour in the middle ear.

In order to better analyse the effect of squeezing CTN against the incus, an additional simulation was performed. This way, a pressure was applied directly in the CTN, in order to simulate the effect of the tumour. This way, the influence of pushing CTN against the incus could be properly studied. The used values of pressure were the same as the ones used in the previous simulations, 174 and 1 300 Pa, being the results analysed for the two nodes close to the incus, D and E.

Chapter 4

Results

A dynamic study was conducted, for a frequency band between 100 Hz and 10 kHz, for 60 and 80 dB SPL, applied in the TM. Once the desired simulations were performed, the obtained results were analysed. The steady state response was obtained, being the displacements of a central node of the stapes footplate as well as a node in the umbo, in the central part of the TM, compared for the different simulated conditions.

Initially, the healthy case (without tumour) was analysed and compared with former studies. Then, the tumours were added to the model and the displacements were compared with the ones obtained for the healthy case. This way, the effect of cholesteatoma development on hearing was assessed before (umbo) and after (footplate) sound transmission along the ossicular chain. The result of modifying the tumour properties, so it became a harder and denser structure, was also a matter of study. The ossicles degradation caused by these tumours was simulated by assigning tumour properties to a part of the ossicles. Finally, the phase angle of the displacement was analysed for the healthy case, small, medium and large tumours, large tumour with properties similar to the ossicles and large tumour with ossicles degradation simulation.

Regarding CTN, the Von Mises stresses were analysed and compared for three different locations, one of them in the CTN location that was pushed down by the tumour and the others in the area where the CTN interacts with the incus, one in the face of CTN that directly interacts with this ossicle and the other in the opposite side. The effects of the medium and the large tumours were analysed. Finally, a pressure was applied directly in the CTN and the effects of this situation were studied.

4.1 Effects of cholesteatoma development in the middle ear on hearing

The results of the obtained displacements for a sound pressure level of 80 dB SPL in the healthy case were compared with the values obtained by other authors in previous studies, in order to validate the model. These results are presented in Figure 4.1. Huber et al. [78], Nishihara et al. [79], Gan et al. [80] and Liu et al. [81] studied the hearing function using a finite element model.

In their research, these groups analysed the displacement of the umbo and stapes footplate, for 80 dB SPL.

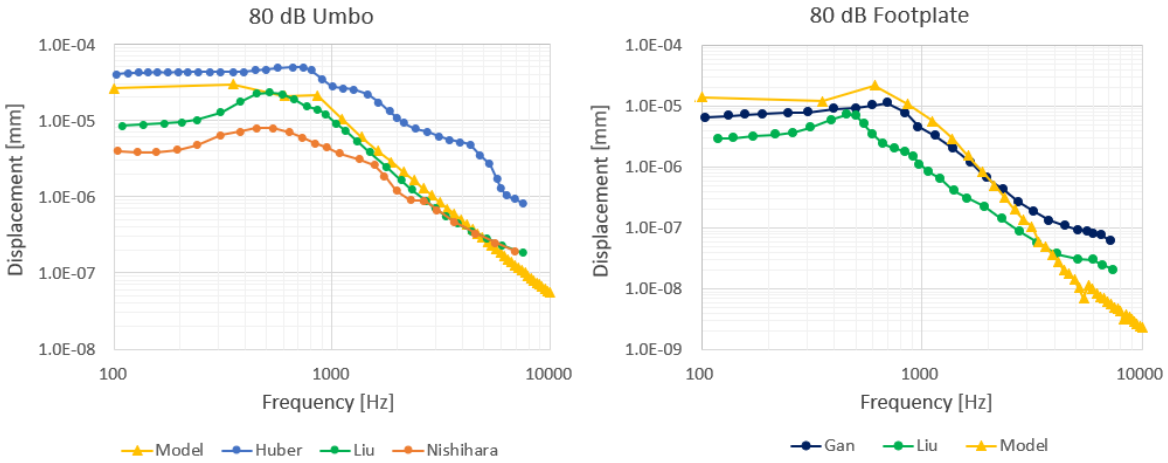

Figure 4.1: Umbo and footplate displacements for 80 dB SPL, obtained by different authors.

Through the results presented in Figure 4.1 it is possible to observe that the used model has a similar behaviour to other biomechanical models of the ear. In what concerns the umbo, the presented values by Liu et al. [81] and Nishihara et al. [79] are slightly lower than the ones of the present model, specially for low frequencies, while the results of Huber et al. [78] are higher than the ones obtained through the used model for all the analysed frequency band. For the footplate displacements, the model used in this project shows higher displacements for lower frequencies and, approximately from 3 kHz, lower displacements than the other models. The observed differences may be due to the discrepancy between some of the modeled structures values and dimensions regarding the literature values.

After validating the used model, the difference between applying 60 dB SPL or 80 dB SPL in the TM was analysed. These values correspond to 2.0×10^{-2} Pa and 2.0×10^{-1} Pa, respectively. The displacements of the umbo and footplate are plotted for these two values in Figure 4.2.

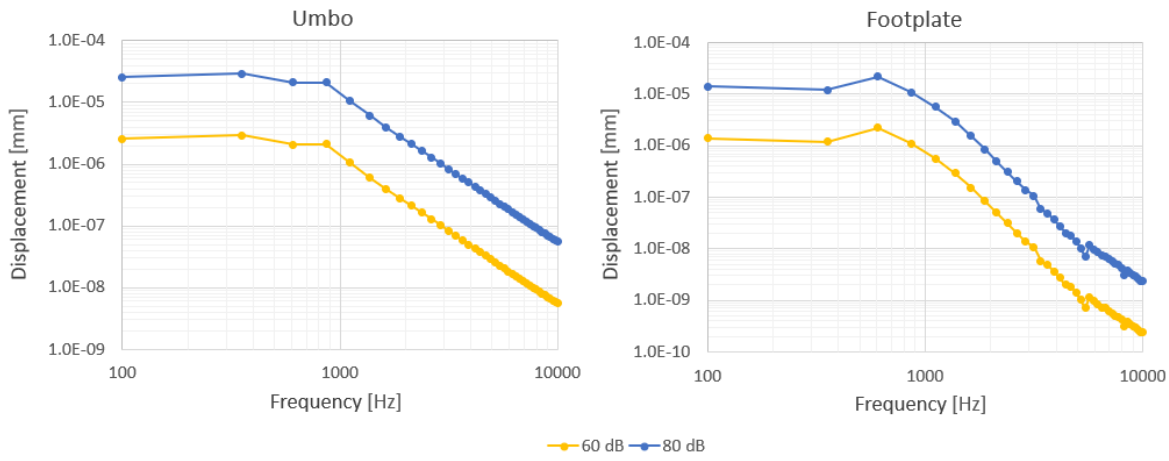

Figure 4.2: Umbo and footplate displacements for 60 and 80 dB SPL.

As it would be expected, the obtained values are proportional to the applied sound pressure, being the ones related to 80 dB SPL ten times superior to the ones for 60 dB SPL. The higher displacements occur for low frequencies. In the umbo, the displacements are approximately constant between 100 and 800 Hz, with values between 2.0×10^{-5} and 3.0×10^{-5} mm for 80 dB SPL, starting to decrease afterwards. In what concerns the footplate, the higher displacements occur, once again, for lower frequencies, with a small peak for 600 Hz, which is associated to a 2.0×10^{-5} mm displacement, for 80 dB SPL. The same behaviour can be observed for 60 dB SPL, with displacements 10 times lower for all frequencies.

Figure 4.3 shows the comparison for the 4 different scenarios studied in this dissertation, healthy ear and small, medium and large tumours, for 60 dB SPL.

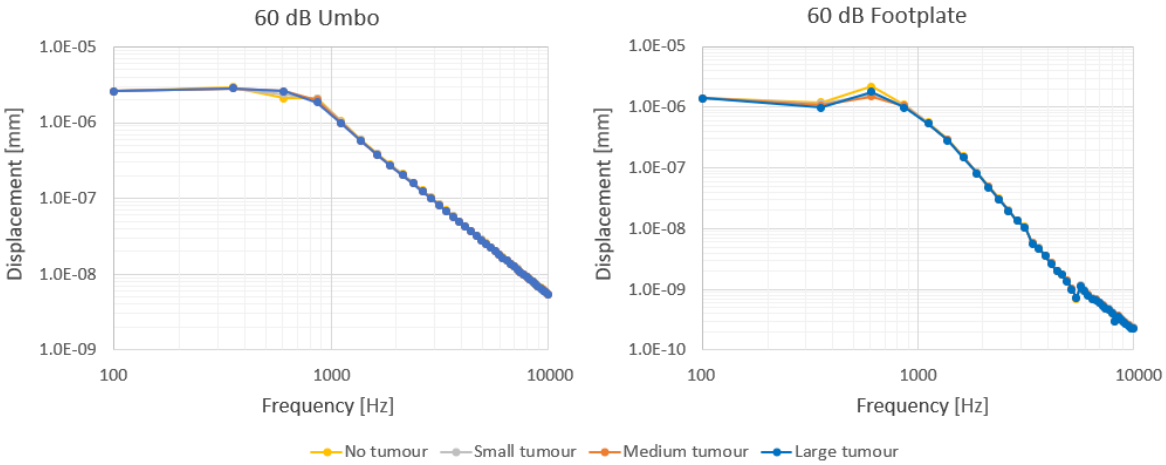

Figure 4.3: Umbo and footplate displacements for healthy case and the three tumour sizes for 60 dB SPL.

For the umbo, the displacements are highly similar for the four cases, usually with a decrease as the tumour develops. The major difference happens around 600 Hz, where the healthy case is associated to the lowest displacement value, which goes against what happens for the majority of frequencies, where the situation without tumour has the higher displacement value. Therefore, this point was disregarded for not conveying relevant information. For the footplate, the values are also extremely close to each other, although there is a decrease in the displacement as the tumour appears and grows. The major difference happens, once again, for low frequencies, mainly around 600 Hz. For these frequencies, it is possible to observe that the case with no tumour has the higher displacement and the values for the three tumours are highly close, being the medium tumour the one with lower displacement. Although this is not expected, as the larger tumour should be the one to cause greater difference, this only happens for this point, while, for the majority of the studied frequencies, the lower displacements are connected to the larger tumour. Nevertheless, the tumour simulations are, as anticipated, connected to lower displacements than the healthy one. The values obtained for the footplate are more relevant than the ones obtained for the umbo, as the footplate is located at the end of the ossicular chain, after sound being transmitted through the ossicles, where the tumour is placed. Therefore, the influence of the cholesteatoma will have greater impact in

this section than in the umbo. The displacement in the footplate allows to understand the amount of sound information that will proceed to the inner ear and, so, reach the brain.

An analogous analysis can be done for the displacements obtained for 80 dB SPL. Figure 4.4 shows the obtained values for the umbo and the footplate. The values are equivalent to the ones obtained for 60 dB SPL, but 10 times higher, as expected. It is important to underline that these first simulations intended to study the influence of cholesteatoma presence and its growth, having the three tumours the same properties and not including any effect on the ossicles. These simulations are far from real life conditions. Nevertheless, they were considered useful as a first approach to study damping phenonena due to tumour development in the middle ear.

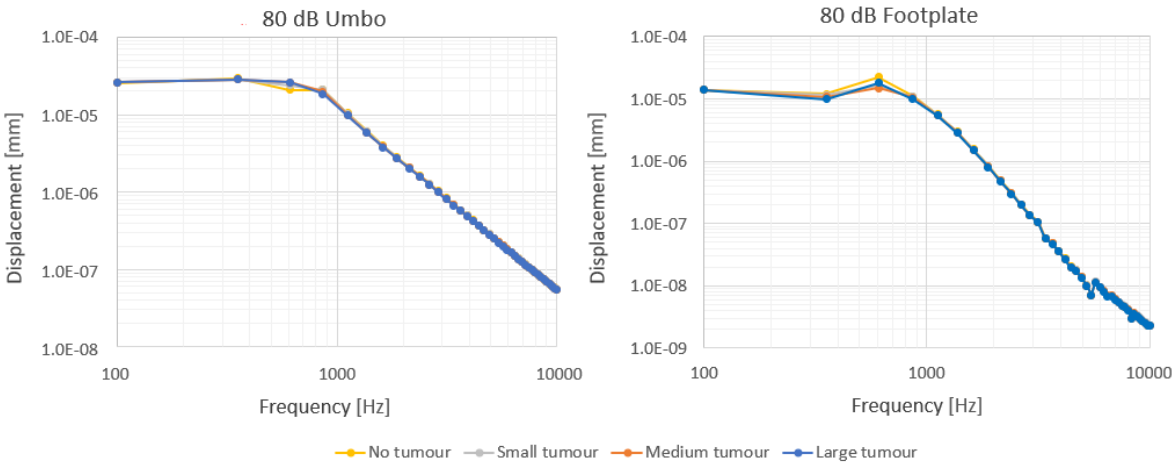

Figure 4.4: Umbo and footplate displacements for healthy case and the three tumour sizes for 80 dB SPL.

The following results are from the simulations with the larger tumour having properties similar to the ossicles. As cholesteatomas change their mechanical properties along time, becoming harder and denser as they grow, the large tumour properties were adjusted to be comparable to the ones of the ossicles. The difference in what concerns the displacements is more visible through this simulation. The results for 60 dB SPL are shown in Figure 4.5 and the analogous results for 80 dB SPL in Figure 4.6. In these graphs, three curves are plotted, the one related to the normal state, no tumour, the one that concerns the large tumour with the originally defined mechanical properties, large tumour 1, and the one regarding the large tumour with properties similar to the ossicles, large tumour 2. The difference is higher for low frequencies, but for the all analysed frequency band it is possible to see greater displacement differences for the tumour with properties similar to the ossicles in comparison to the healthy state.

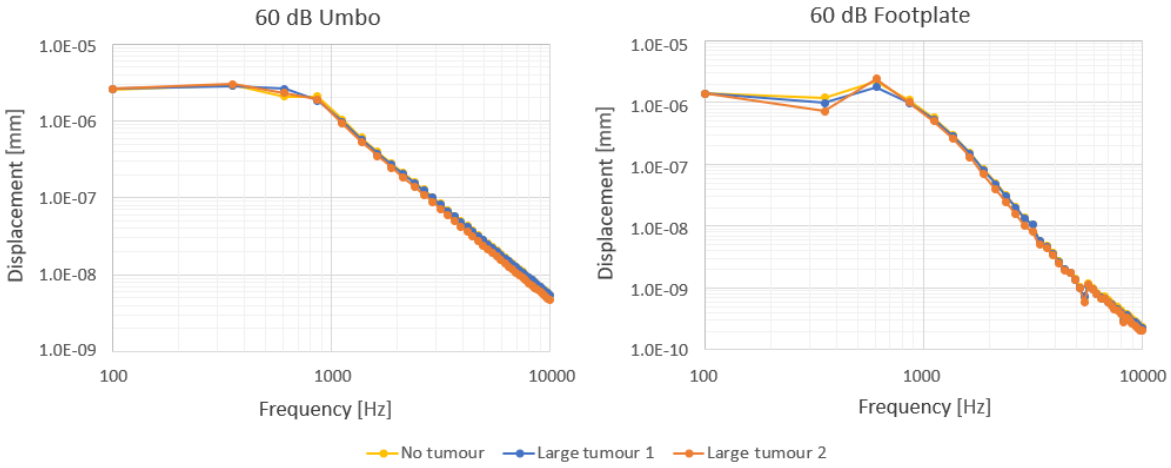

Figure 4.5: Umbo and footplate displacements for healthy case and the large tumour considering normal tumour properties and tumour properties similar to the ossicles for 60 dB SPL.

For 80 dB SPL, the results are analogous, as one can see in Figure 4.6. This data sustains the idea that the cholesteatoma properties evolve along time, as people with cholesteatoma sometimes realise they have this condition when they start to experience hearing loss, so the difference in terms of footplate displacement should be higher than the ones plotted in Figures 4.3 and 4.4. Further studies exploring different properties, that confer different behaviour to the tumour, transforming it in a harder and denser structure but having properties that not the ossicles' would be of interest.

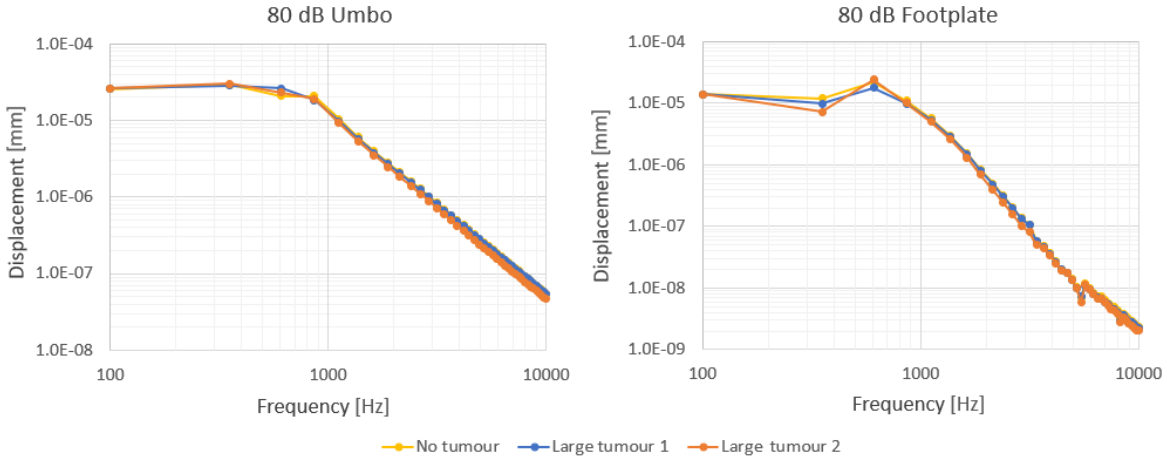

Figure 4.6: Umbo and footplate displacements for healthy case and the large tumour considering normal tumour properties and tumour properties similar to the ossicles for 80 dB SPL.

The next simulation was the one that considered ossicles degradation. This simulation resembles more with the real scenario, where cholesteatomas have the ability to recruit osteoclasts due to the inflammatory reaction they trigger, and degrade the ossicles. This way, Figures 4.7, 4.8 and 4.9, that concern the small, medium and large tumours, respectively, show the results of the simulation including bone degradation. In these tests, the mechanical properties of the ossicles' elements that were wrapped by the tumour (incudomalleolar joint and part of the malleus and the

incus) were modified to have the same properties as the tumour. In these graphs, the displacements for the umbo and the footplate for 60 dB SPL are presented for the different tumour sizes. The results are compared between each tumour, for the case in which ossicle degradation is not considered and for the degradation simulation.

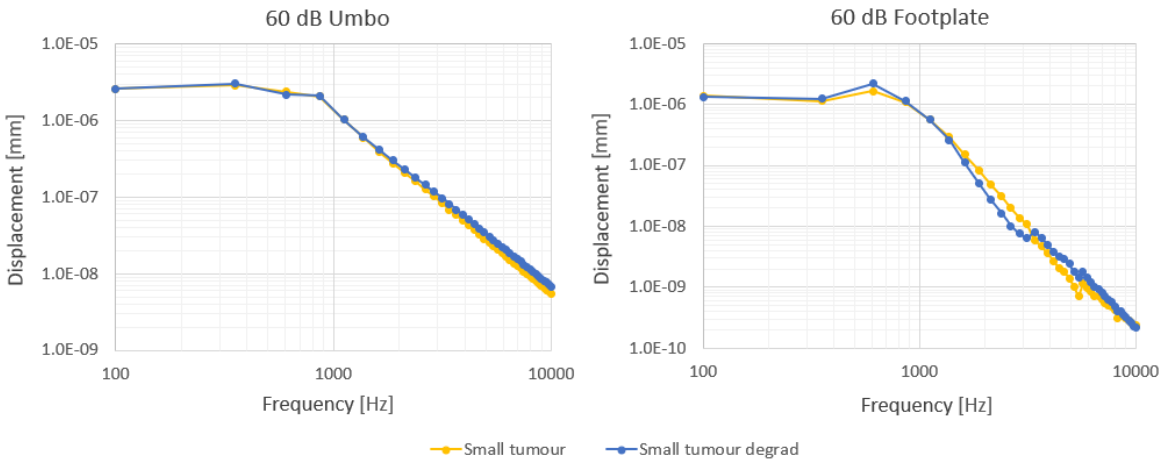

Figure 4.7: Umbo and footplate displacements in the small tumour simulation considering normal ossicles properties and tumour degradation, for 60 dB SPL.

Regarding the results for the small tumour, the displacements registered in the umbo show few variation. The values obtained for the footplate are slightly different for the simulation of ossicle degradation when comparing with the case without degradation. For low frequencies, the displacement is a bit higher than the registered for the small tumour without degradation. For high frequencies, the opposite happens, the displacements are slightly lower for the case in which degradation is considered.

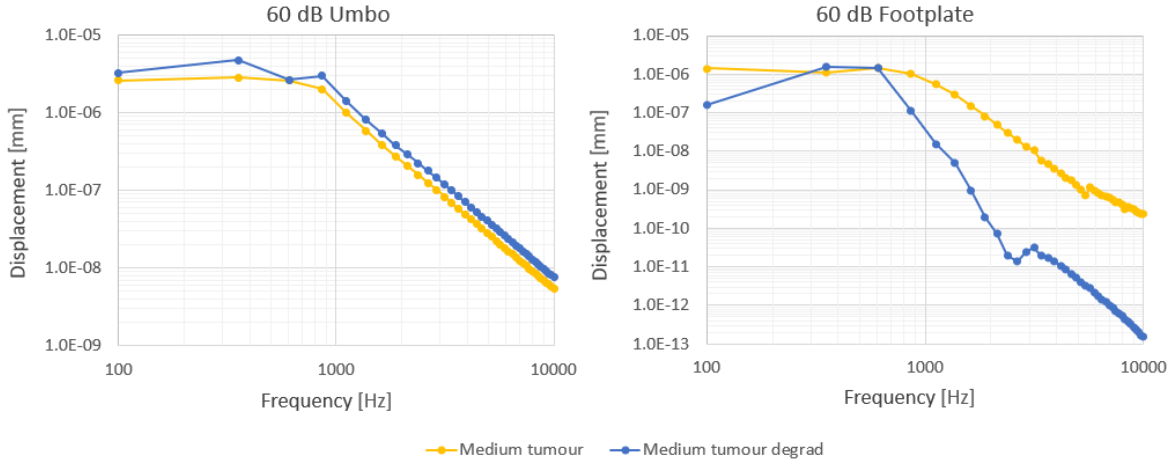

Figure 4.8: Umbo and footplate displacements in the medium tumour considering normal ossicles properties and tumour degradation, for 60 dB SPL.

For the medium tumour, the results are slightly different. The umbo displacements for the degradation simulation are higher for all the frequency band. Although at first it may not make

sense, this might be explained by the fact that the ossicular chain becomes softer and less dense when degradation is considered and so it offers less resistance to vibrations, leading to a higher displacement of the umbo. On the other hand, the footplate displacements are generally lower for the case where degradation is considered, which was expected as a softer material will not favour the conduction of sound information.

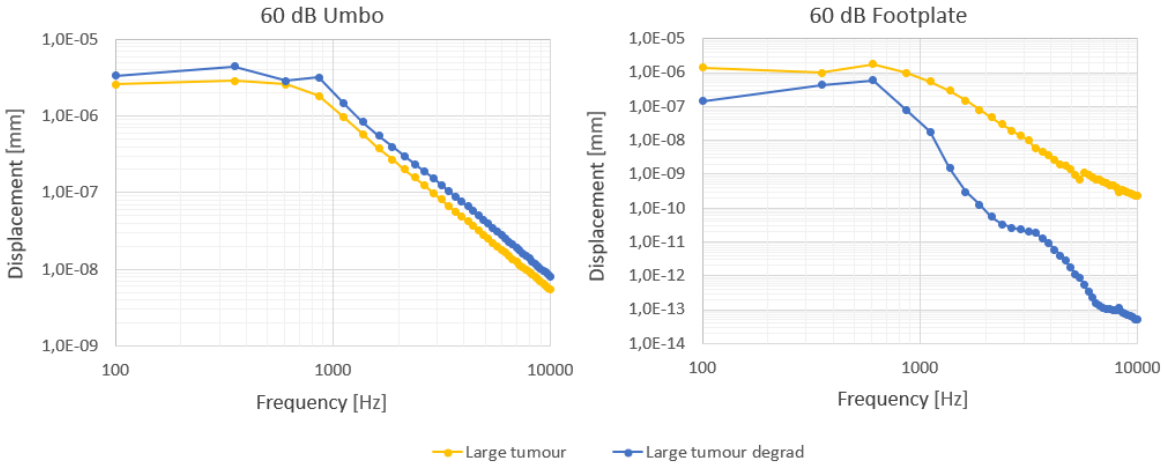

Figure 4.9: Umbo and footplate displacements the large tumour considering normal ossicles properties and tumour degradation, for 60 dB SPL.

For the large tumour, the values obtained for the umbo are similar the ones in the medium tumour simulations. The case in which degradation was considered records higher displacements than the case without degradation. The values obtained for the footplate are lower for the degradation simulation, for all frequencies. This difference is considerably high for higher frequencies, being the displacements around 10^4 times smaller for the degraded ossicles.

Figures 4.10, 4.11 and 4.12 show the results for the correspondent simulations for 80 dB SPL. The obtained values are extremely similar, with the expected difference of being 10 times superior. The differences that may be observed result from the selection of the elements for property alteration having been performed manually for the several cases. Although this was an interesting process to study, there is room for improvement. In the current work, the performed analysis simulated that the tumour had the ability to degrade the ossicles and completely replace the degraded portions. Nevertheless, an intermediate simulation, in which only some portions of the ossicles would be altered instead of all the part of the ossicles involved by the tumour, would be of interest, so several degrees of degradation could be studied. Furthermore, as the osteoclasts activity completely degrades the ossicles, it is possible that the degraded parts are not replaced by the tumour. In this case, the ossicular chain could be interrupted, which would lead to severe conductive hearing loss. A simulation of this condition, where some parts of the ossicles would be removed to better reproduce osteoclasts activity would also be interesting.

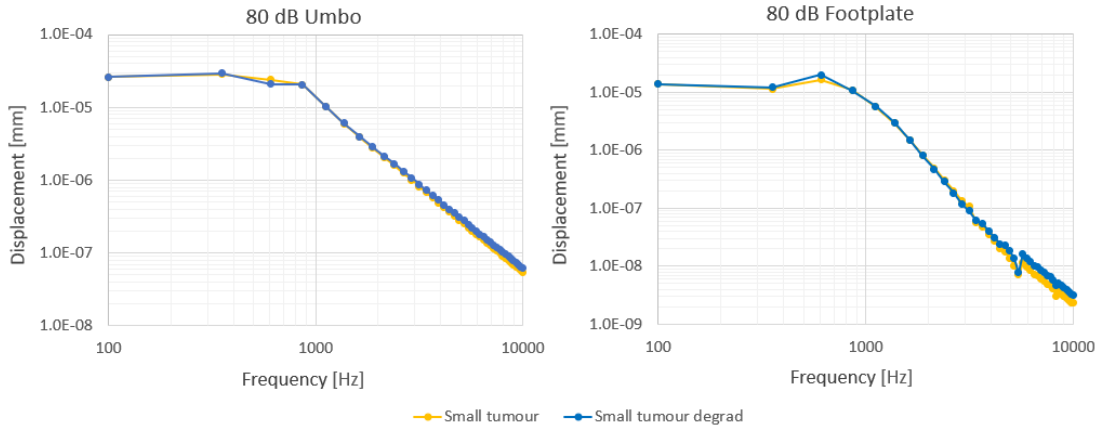

Figure 4.10: Umbo and footplate displacements for the small tumour considering normal ossicles properties and tumour degradation, for 80 dB SPL.

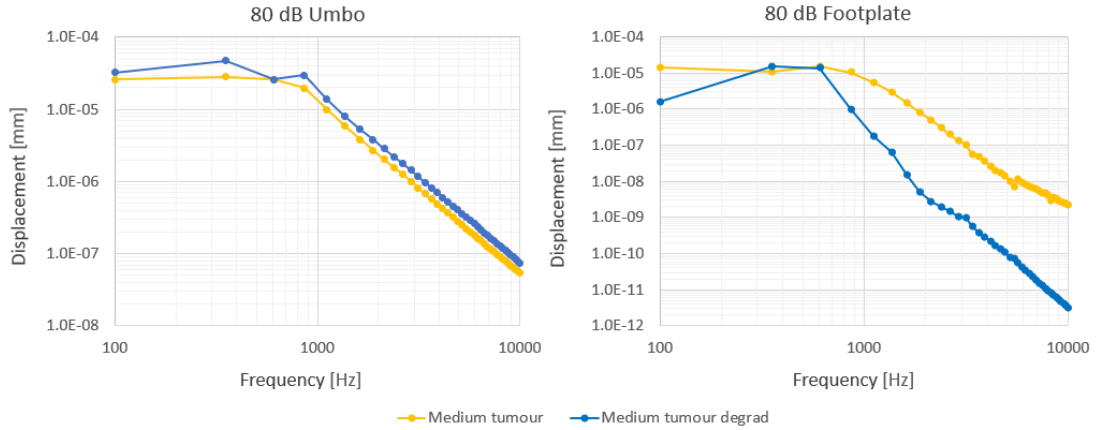

Figure 4.11: Umbo and footplate displacements for the medium tumour considering normal ossicles properties and tumour degradation, for 80 dB SPL.

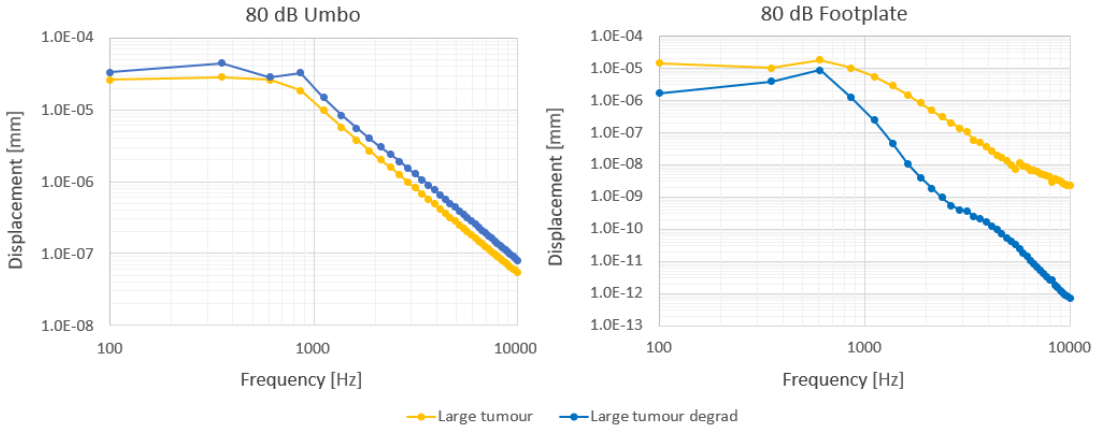

Figure 4.12: Umbo and footplate displacements for the large tumour considering normal ossicles properties and tumour degradation, for 80 dB SPL.

The phase angle of the displacement was compared for the different studied situations. Figure 4.13 shows these results for the healthy case and the three cholesteatoma sizes with tumour properties. In general, it is possible to see that the phase angle of the umbo displacement is nearly constant until 200 Hz, ranging between 160 and 180 degrees. From this frequency on, it shows two minimums between 200 and 300 Hz, with angles between 130 and 150 degrees, and a peak between 300 and 400 Hz, with a phase angle between 200 and 220 degrees. From 400 to 700 Hz, the angle does nor suffer major variations, being its value between 150 and 180 degrees. Finally, there is an increase of the angle until 1 kHz and then the angle remains approximately constant until 10 kHz, around 220 and 250 degree. Regarding the footplate, it is possible to observe that there is a small peak between 200 and 300 Hz, with the angle rising from around 110/120º to 160/170º. A minimum appears next, between 400 and 500 Hz, with the phase angle decreasing to between 50 and 70 degrees. The greater peaks occur for frequencies between 500 and 700 Hz, being the greater registered angle 280 degrees. Finally, there is a decrease and the phase becomes almost constant for frequencies between 2 and 10 kHz. It is possible to observe a shift to the left as the tumour grows, for both the umbo and the footplate, especially for low frequencies.

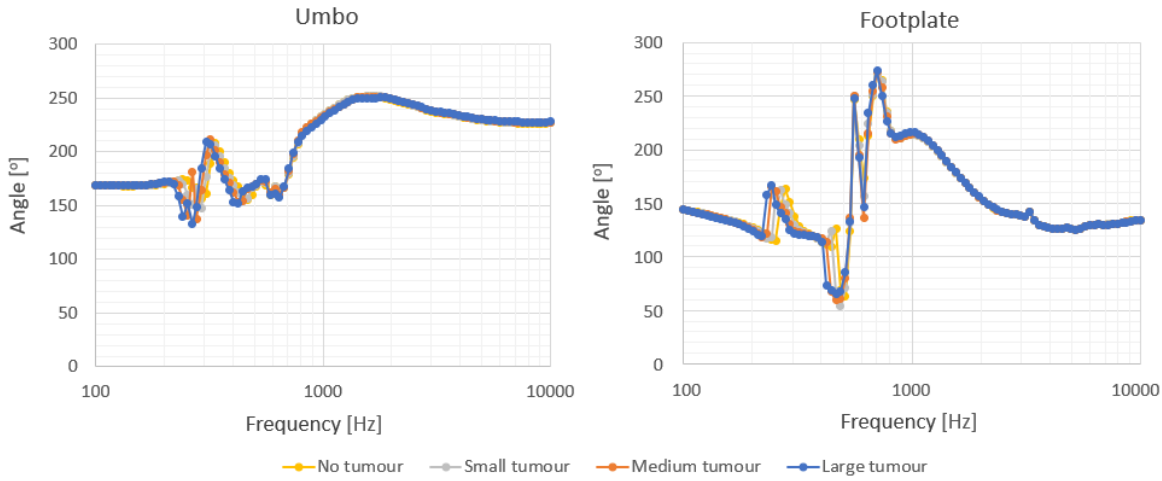

Figure 4.13: Phase response of the umbo and footplate for the healthy case and the three tumours.

The phase angle of the displacement was also analysed for the large tumour with properties similar to the ossicles. Figure 4.14 shows the obtained values for the large tumour simulations with the standard properties and the bony material properties. For the umbo, it is possible to see a shift to the left in all the studied frequencies for the tumour with properties similar to the ossicles. In what concerns the footplate, a similar delay is observed, just in low frequencies, until around 500 Hz. From this point on, the values for the two simulations almost overlap.

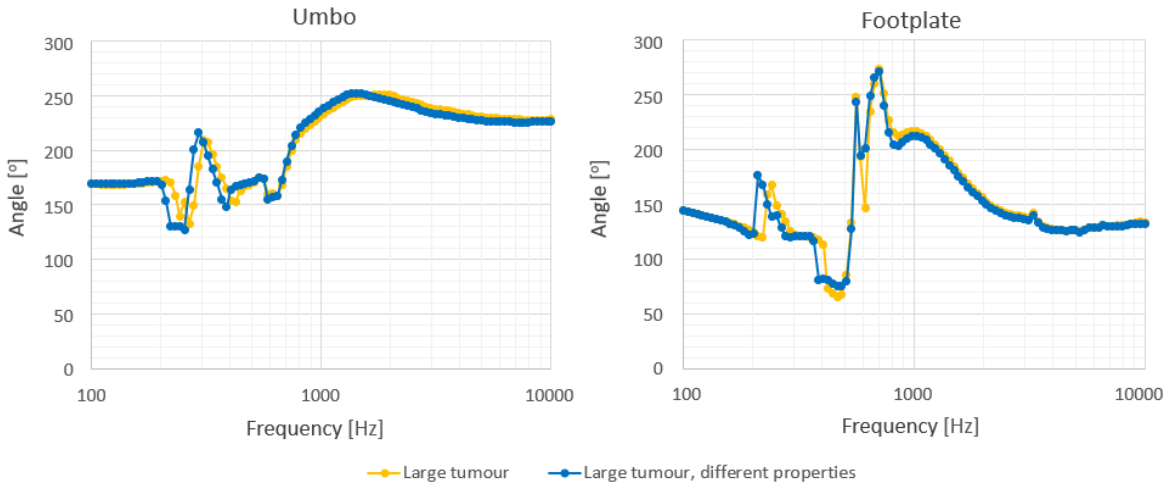

Figure 4.14: Phase response of the umbo and footplate for the large tumour considering standard properties and properties similar to the ossicles.

Finally, the phase response for the regular large tumour and the large tumour considering ossicle degradation was compared, being the results present in Figure 4.15. For the umbo, the general shape of the graph related to the ossicles degradation is similar to the one related to the case where degradation is not considered. Nevertheless, there are some differences that do not occur in other analysed conditions. Unlike what happened for the other simulations, the shape of the phase response changes considerably for the footplate, in the degradation scenario. The graph related to this simulation is characterized by a great amount of steep peaks and valleys.

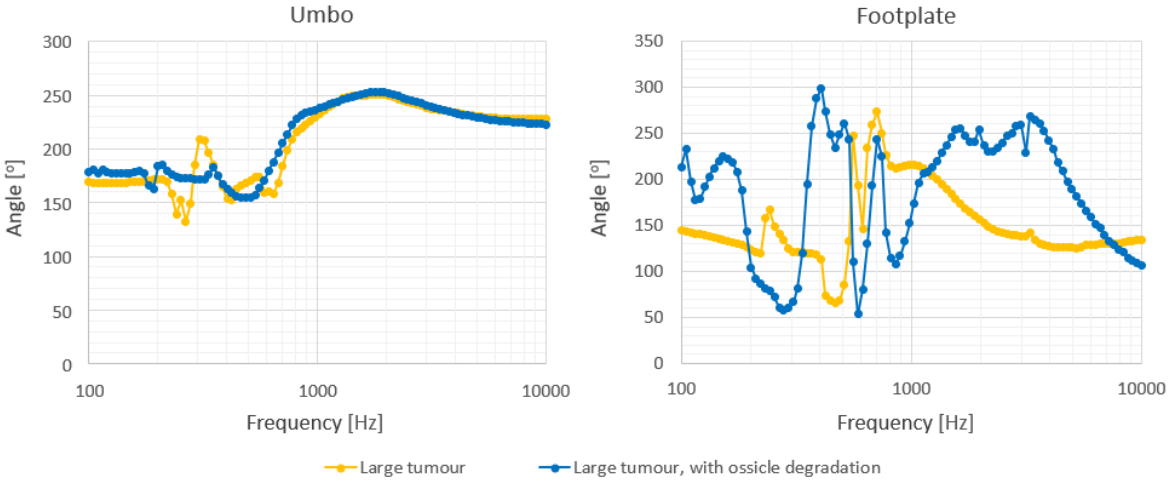

Figure 4.15: Phase response of the umbo and footplate for the large tumour considering regular properties and ossicles degradation.

4.2 Effects of cholesteatoma development in chorda tympani nerve

The cholesteatoma influence in what concerns CTN and possible FP was also evaluated. Initially, this was tested by expanding the tumours towards the CTN. Then, the effect of pressuring

CTN was studied by directly applying pressure on its surface.

The first simulation regarding the effects of the cholesteatoma growth in CTN was performed for the medium tumour, as this way it would be possible to recreate the first interaction between CTN and the cholesteatoma. The effects of applying an internal pressure of 174 Pa on the shell was assessed. The values were obtained for three specific nodes, C, a central node in the part of the CTN that first interacts with the cholesteatoma, being pushed down by the tumour, D, a node that belongs to the portion of CTN that passes close to the incus, in the side that does not contact with the ossicle, and E, a node of CTN that contacts with the incus. Table 4.1 shows the Von Mises stress obtained for these three nodes.

Table 4.1: Von Mises stress obtained for the CTN when affected by the medium tumour.

Nodes	***C***	***D***	***E***
Von Mises Stress (Pa)	94699.4	217012	334652

It is possible to observe that the higher stress value occurs for the node that contacts with the incus. Although node C is closer to the pressure source (the cholesteatoma), this part of the CTN can move freely without any other structure blocking its movement. This way, the higher stresses will be related to the node that contacts with the incus, as this ossicle blocks CTN movement. Figure 4.16 shows the stress distribution in the CTN.

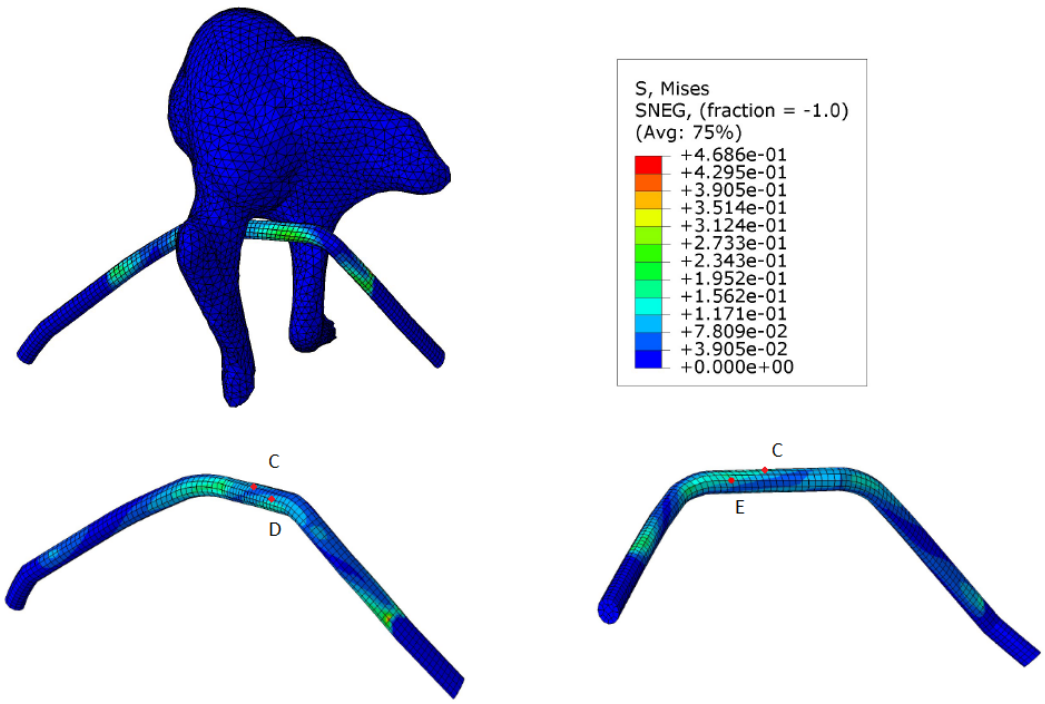

Figure 4.16: Von Mises stress obtained for the CTN when affected by the medium tumour.

The large tumour influence on CTN was then studied. Table 4.2 shows the Von Mises stress obtained for the three nodes, for a pressure of 1 300 Pa.

Table 4.2: Von Mises stress obtained for the CTN when affected by the large tumour.

Nodes	***C***	***D***	***E***
Von Mises Stress (Pa)	89064	181840	404098

It is possible to observe that, once again, the grater stress value happens for the node in contact with the incus. In general, it would be expected that the stress values resulting from the analysis of the effect of the large tumour were higher than the ones obtained for the medium tumour, which does not happen. Nevertheless, it is important to take into consideration that the tumour shape may have influence. This way, and as the large tumour had to be adjusted to the CTN, its lower face is not flat as it is the one of the medium tumour. The irregularity of the large tumour lower surface may be the reason why the applied internal pressure does not lead to higher stresses. An image of the stress distribution in the CTN can be seen in Figure 4.17.

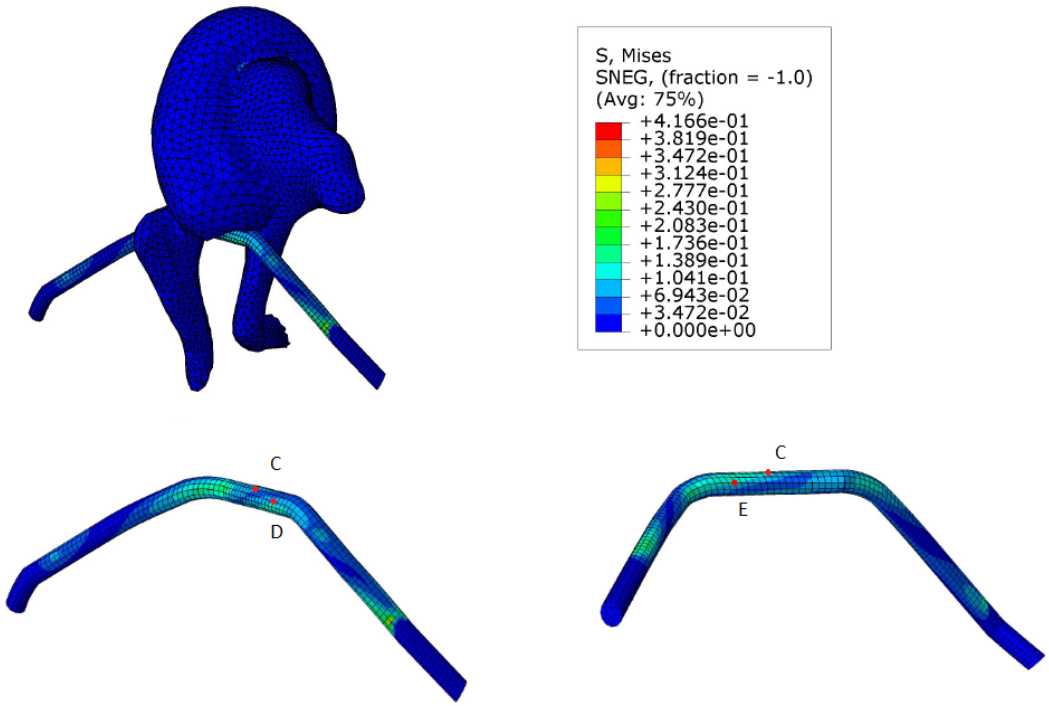

Figure 4.17: Von Mises stress obtained for the CTN when affected by the large tumour.

Finally, the effect of applying a pressure directly on the CTN surface was studied. The applied pressures were the same as in the two cases explained above. The results are in Table 4.3. It is possible to observe that the stress is higher when a higher pressure is applied, being this difference more relevant in node E, the node that contacts directly with the incus. This may be explained by the fact thar this node has a fixed barrier to stop its movement, the incus, which causes a higher stress on it.

As no former studies were found regarding this topic, it was not possible to compare these results with literature values. Thus, the obtained results only allow to infer on possible outcomes for CTN deformation. As CTN crosses the middle ear close to the ossicles, tumour growth near

Table 4.3: Von Mises stress obtained for the CTN when pressure is directly applied on its surface.

Nodes	***D***	***E***
Von Mises Stress (Pa) for an applied pressure of 174 Pa	217017	337067
Von Mises Stress (Pa) for an applied pressure of 1300 Pa	217054	352899

this structure will probably smash the CTN against one of the ossicles, leading to higher tensions in CTN. Being squeezed by the cholesteatoma against the incus may lead to taste aberrance and, eventually, FP, if the pressure on CTN is high. Nevertheless, the presented studies in Chapter 2 suggest that these symptoms are likely to disappear when pressure fades away. Furthermore, it was possible to conclude that a cholesteatoma that grows in the same site as the one simulated in this work starts to directly interfere with CTN from the moment it has a dimension slightly superior to the medium tumour.

Chapter 5

Conclusion and future work

The auditory system plays an important role in people's lives, as it is responsible for hearing. The nerves that cross the ear or regions near this organ work in perfect symbiosis with the ear mechanisms. However, some conditions may interfere with the ear activities. COM may compromise human health, as it can affect several processes that occur inside or even around the ear. On the one hand, it can damage hearing, by affecting the ossicular chain or filling the tympanic cavity with products resulting from the inflammatory process. On the other hand, it can affect ear or brain structures, namely nerves, leading to nefarious consequences.

The middle ear behaviour was studied in this thesis for a frequency band between 100 and 10 000 Hz, for 60 and 80 dB SPL. The effects of cholesteatoma development around the incudomalleolar joint and, more specifically, affecting the CTN, were evaluated through the development of a computational model of these structures, using FEM. The displacements of the umbo and the stapes footplate were obtained and compared for several different simulated conditions. The obtained results suggest that the sound information that proceeds to the inner ear decreases as the tumour appears and grows. The fact that the cholesteatoma properties evolve along time contribute to higher damping phenomena, resulting in even less information reaching the stapes. When ossicles degradation is considered, there is a higher variation in the results, keeping the trend of hampering hearing.

Regarding CTN, the fact that this structure runs uncovered in the middle ear makes it more susceptible to the events that occur there. The tumour growth towards CTN was simulated and the Von Mises stresses were analysed in several locations of the CTN. The obtained stresses show that the fact that CTN is positioned between two ossicles leads to the possibility of smashing it against a fixed structure and so, greater tensions. This allows taste disturbance and, possibly, facial paralysis.

In what concerns future work, it would be interesting to test an intermediate state of degradation for the ossicles. In this work, to simulate this phenonenon, all the elements that belong to the malleus, incus and incudomalleolar joint that were wrapped by the cholesteatomas were modified, changing their mechanical properties so that their material was the same as for the tumours. It would be advantageous to study what would happen if only some clusters of elements of the same

region were modified.

Additionally, as osteoclasts degrade bone, the parts of the ossicles affected by these cells would, in a real scenario, disappear. This way, not only the part of the ossicles enfold in the cholesteatoma would be affected and replaced by the tumour itself, but some parts of the ossicles would be completely destroyed, which would lead to a greater conductive hearing loss. This would also be a reliable and useful simulation.

An analysis in which tumour growth could be mimicked in a more accurate way instead of only three tumour sizes would provide more information. Moreover, it would be useful to compare the obtained results with audiograms of patients suffering from this condition, in order to better assess which frequency bands experience greater variations when comparing with a healthy ear and to better establish the relation between cholesteatoma growth and hearing loss.

Furthermore, it would be meaningful to conduct a similar study as the current one using an available more complete model of the ear, that includes air in the tympanic cavity. The air mesh would have to be adjusted to the new structures, CTN and the three different sized tumours, and then, the simulations would be performed. It would be interesting to compare the results of that more complex model with the results obtained in this project.

Appendix A

CTN reported values

Cadaver identification number	Section of chorda tympani nerve			Total length
	Section 1 Mastoid process	Section 2 Tympanic cavity	Section 3 Submandibular fossa	
875604	11.95	13.00	29.12	54.07
876302	9.93	9.04	33.26	52.23
876506	4.54	9.97	30.13	44.64
881501	11.65	9.04	33.30	53.99
8802	5.71	8.01	39.27	52.99
8823	8.99	9.87	39.54	58.40
8274	14.12	9.34	42.90	66.36
882401	13.38	9.62	29.19	52.19
8803	12.73	9.43	52.42	74.58
8697	2.79	11.27	28.87	42.93
8750	6.23	9.56	35.84	51.63
881601	14.18	7.86	32.93	54.97
8814	6.16	11.16	35.84	53.16
8849	6.21	10.14	36.09	52.44
8810	9.26	10.34	30.37	49.97
8850	6.29	9.68	40.31	56.28
Mean	9.01	9.83	35.59	54.43
SD	3.68	1.24	6.28	7.49

Figure A.1: CTN measured values in the study of Liu et al. [14].

Appendix B

Middle ear before and after the addiction of CTN

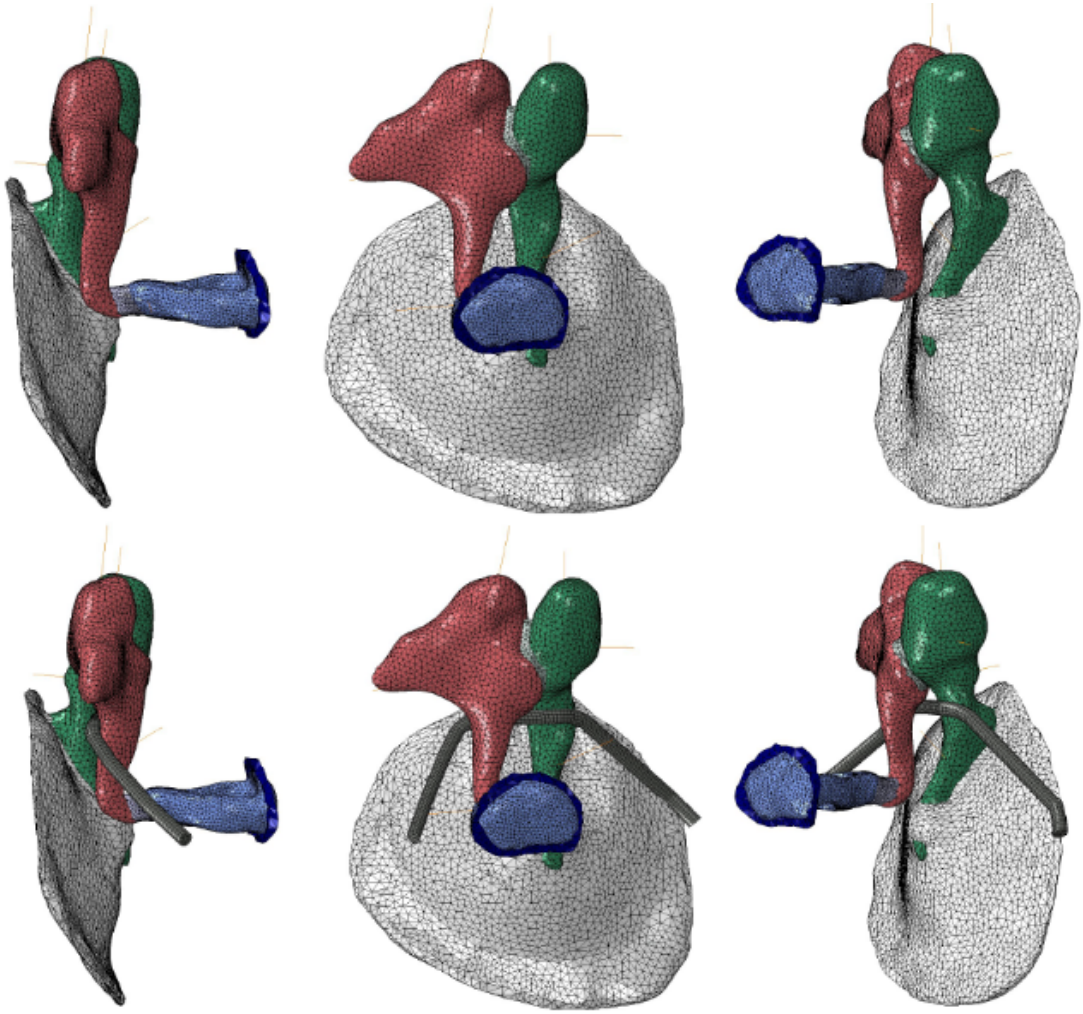

Figure B.1: Middle ear with and without CTN

References

[1] Peter S Morris and Amanda J Leach. Acute and chronic otitis media. *Pediatric Clinics*, 56(6):1383–1399, 2009.

[2] Minoru Ikeda, Hidehisa Nakazato, Keiko Onoda, Ryoji Hirai, and Akinori Kida. Facial nerve paralysis caused by middle ear cholesteatoma and effects of surgical intervention. *Acta oto-laryngologica*, 126(1):95–100, 2006.

[3] LMJ Lips, PJ Nelemans, FMD Theunissen, E Roele, J van Tongeren, JR Hof, and AA Postma. The diagnostic accuracy of 1.5 t versus 3 t non-echo-planar diffusion-weighted imaging in the detection of residual or recurrent cholesteatoma in the middle ear and mastoid. *Journal of Neuroradiology*, 2019.

[4] Rodrigo Duzanowski Savaris. Study on dynamic behavior on the human ear with the presence of an irregular body. *Master Thesis. Porto, Portugal: Faculdade de Engenharia da Universidade do Porto*, 2018.

[5] Carmen L McKnight. Vibratory response of dry human skulls. *Master Thesis. Nova Scotia, Canada: Dallhousie University*, 2012.

[6] Maria Fernanda Gentil Costa. Estudo biomecânico do ouvido médio. *PhD Dissertation. Porto, Portugal: Faculdade de Engenharia da Universidade do Porto*, 2008.

[7] Bruno André Faria Areias. Simulação biomecânica do ouvido humano, incluindo patologias do ouvido médio. *Master Thesis. Porto, Portugal: Faculdade de Engenharia da Universidade do Porto*, 2014.

[8] Marco da Costa Marques. Estudo biomecânico para a reabilitação do ouvido médio humano. *Master Thesis. Porto, Portugal: Faculdade de Engenharia da Universidade do Porto*, 2012.

[9] N Wendell Todd and Francis X Creighton Jr. Malleus and incus: correlates of size. *Annals of Otology, Rhinology & Laryngology*, 122(1):60–65, 2013.

[10] Ernest Glen Wever and Merle Lawrence. *Physiological acoustics*. Princeton University Press, 2015.

[11] Richard Drake, A Wayne Vogl, and Adam WM Mitchell. *Gray's Anatomy for Students-Rental: With STUDENT CONSULT Online Access*. Elsevier Health Sciences, 2009.

[12] Barry J Anson, James A Donaldson, Raymond L Warpeha, and Michael J Rensink. The facial nerve, sheath and blood supply in relation to the surgery of decompression. *Annals of Otology, Rhinology & Laryngology*, 79(4):710–727, 1970.

[13] Bruce Proctor. The development of the middle ear spaces and their surgical significance. *The Journal of Laryngology & Otology*, 78(7):631–645, 1964.

[14] Longping Liu, Robin Arnold, and Marcus Robinson. Dissection and exposure of the whole course of deep nerves in human head specimens after decalcification. *International journal of otolaryngology*, 2012, 2012.

[15] Erlo Esslen. Investigations, part ii: Electrophysiologic investigations on the natural history of acute facial palsies. In *The Acute Facial Palsies*, pages 39–116. Springer, 1977.

[16] M.; Moreira A.P.; Lima M.O.; Parreiras L.P. Parreiras. *Anatomia do nervo facial e etiologia da paralisia facial periférica*. Revista Digital Buenos Aires, N^{o} 146, 2010.

[17] M. May. *The facial nerve*. Thieme Inc, USA, 1986.

[18] Henry Gray. *Gray's anatomy: with original illustrations by Henry Carter*. Arcturus Publishing, 2009.

[19] JVD Hough. Malformations and anatomical variations seen in the middle ear during the operation for mobilization of the stapes. *The Laryngoscope*, 68(8):1337–1379, 1958.

[20] B Minnigerode. Intratympanale aufzweigung der chorda tympani, eine seltene anatomische verlaufsvariante. *Acta Oto-Laryngologica*, 59(1):20–22, 1965.

[21] Charles Kent Smith, Felix R Portelli, Lee K Hermann, and Joseph W Walike. Facial palsy caused by facial nerve tumor. *The Laryngoscope*, 81(9):1542–1545, 1971.

[22] P Gopalan, M Kumar, D Gupta, and JJ Phillipps. A study of chorda tympani nerve injury and related symptoms following middle-ear surgery. *The Journal of Laryngology & Otology*, 119(3):189–192, 2005.

[23] Philip Michael and Vivek Raut. Chorda tympani injury: operative findings and postoperative symptoms. *Otolaryngology—Head and Neck Surgery*, 136(6):978–981, 2007.

[24] Matthew PA Clark and Steve O'Malley. Chorda tympani nerve function after middle ear surgery. *Otology & Neurotology*, 28(3):335–340, 2007.

[25] Takehisa Saito, Yasuhiro Manabe, Yoshiyuki Shibamori, Takahiro Yamagishi, Hideki Igawa, Masaharu Tokuriki, Yoko Fukuoka, Ichiro Noda, Toshio Ohtsubo, and Hitoshi Saito. Long-term follow-up results of electrogustometry and subjective taste disorder after middle ear surgery. *The Laryngoscope*, 111(11):2064–2070, 2001.

[26] Jack H Noble, Frank M Warren, Robert F Labadie, and Benoit M Dawant. Automatic segmentation of the facial nerve and chorda tympani in ct images using spatially dependent feature values. *Medical physics*, 35(12):5375–5384, 2008.

[27] Olivier Trost, René-Charles Rouchy, Charles Teyssier, Apolline Kazemi, Narcisse Zwetyenga, Gabriel Malka, Nicolas Cheynel, and Pierre Trouilloud. Ct-scan imaging of iron marked chorda tympani nerve: anatomical study and educational perspectives. *Surgical and radiologic anatomy*, 33(6):515–521, 2011.

[28] Orhan Gedikli, Harun Doğru, Gülsen Aydin, Mustafa Tüz, Kemal Uygur, and Aliye Sari. Histopathological changes of chorda tympani in chronic otitis media. *The Laryngoscope*, 111(4):724–727, 2001.

[29] Katarina Berling, Paula Mannström, Mats Ulfendahl, Niklas Danckwardt Lilliestrom, and Magnus Von Unge. The chorda tympani degenerates during chronic otitis media: an electron microscopy study. *Acta Oto-Laryngologica*, 135(6):542–548, 2015.

[30] Carolina Ana Garbe et al. Estudo biomecânico para reabilitação do ouvido médio humano. *Porto, Portugal: Faculdade de Engenharia da Universidade do Porto*, 2010.

[31] Luis L. Henrique. *Acústica Musical*. Fundação Calouste Gulbenkian, 2002.

[32] M.R. López. *Acústica arquitectónica aplicada*. Paraninfo, 1999.

[33] Thomas Zahnert. The differential diagnosis of hearing loss. *Deutsches ärzteblatt international*, 108(25):433, 2011.

[34] Marie Forséni, Dan Bagger-Sjöbäck, and Malou Hultcrantz. A study of inflammatory mediators in the human tympanosclerotic middle ear. *Archives of Otolaryngology–Head & Neck Surgery*, 127(5):559–564, 2001.

[35] James L Sheeley and William F House. Tympanosclerosis. *Archives of otolaryngology*, 76(2):151–157, 1962.

[36] Saad Asiri, Alaa Hasham, Fatma Al Anazy, Siraj Zakzouk, and Adel Banjar. Tympanosclerosis: review of literature and incidence among patients with middle-ear infection. *The Journal of Laryngology & Otology*, 113(12):1076–1080, 1999.

[37] Gonçalo Manuel Nunes Gomes Pereira. Otosclerose: Etiologia, histologia e fisiopatologia. *Master thesis. Porto, Portugal: Instituto de Ciências Biomédicas Abel Salazar*, 2011.

[38] Jos J Eggermont. *Hearing loss: Causes, prevention, and treatment*. Academic Press, 2017.

[39] Maroeska M Rovers, Anne GM Schilder, Gerhard A Zielhuis, and Richard M Rosenfeld. Otitis media. *The lancet*, 363(9407):465–473, 2004.

[40] American Academy of Pediatrics Subcommittee on Management of Acute Otitis Media et al. Diagnosis and management of acute otitis media. *Pediatrics*, 113(5):1451, 2004.

[41] Ramsey Alsarraf, Chung J Jung, Jonathon Perkins, Catherine Crowley, Nicole W Alsarraf, and George A Gates. Measuring the indirect and direct costs of acute otitis media. *Archives of Otolaryngology–Head & Neck Surgery*, 125(1):12–18, 1999.

[42] Charles J Limb, Lawrence R Lustig, JO Klein, et al. Acute otitis media in adults. *UpToDate Welthem, MA: UpToDate*, 2018.

[43] Lorenzo Monasta, Luca Ronfani, Federico Marchetti, Marcella Montico, Liza Vecchi Brumatti, Alessandro Bavcar, Domenico Grasso, Chiara Barbiero, and Giorgio Tamburlini. Burden of disease caused by otitis media: systematic review and global estimates. *PloS one*, 7(4), 2012.

[44] Jason A Smith and Christopher J Danner. Complications of chronic otitis media and cholesteatoma. *Otolaryngologic Clinics of North America*, 39(6):1237–1255, 2006.

[45] World Health Organization et al. Chronic suppurative otitis media: burden of illness and management options. 2004.

[46] H Haidar, R Sheikh, A Larem, A Elsaadi, H Abdulkarim, S Ashkanani, and A Alqahtani. Ossicular chain erosion in chronic suppurative otitis media. *Otolaryngol (Sunnyvale)*, 5(203):2, 2015.

[47] Kenneth L Kennedy and Achint K Singh. Middle ear cholesteatoma. In *StatPearls*. StatPearls Publishing, 2019.

[48] Mahmood F Bhutta, Ian G Williamson, and Holger H Sudhoff. Cholesteatoma. *Bmj*, 342, 2011.

[49] World Health Organization et al. *Global costs of unaddressed hearing loss and cost-effectiveness of interventions: a WHO report, 2017*. World Health Organization, 2017.

[50] Z Hu and Z Wang. Research of the chorda tympani nerve in cholesteatoma. *Zhonghua er bi yan hou ke za zhi*, 36(2):123–125, 2001.

[51] H Wendt. Ueber ein endotheliales cholesteatom des trommelfelles. *Arch Phys Heilkd Wagner*, 14:551–61, 1873.

[52] T Palva, A Palva, and K Dammert. Middle ear mucosa and chronic ear disease. *Archives of Otolaryngology*, 87(1):3–11, 1968.

[53] J Sade. Treatment of retraction pockets and cholesteatoma. *The Journal of Laryngology & Otology*, 96(8):685–704, 1982.

[54] Meher D Wells and L Michaels. Mode of growth of acquired cholesteatoma. *The Journal of Laryngology & Otology*, 105(4):261–267, 1991.

[55] H Takahashi, H Nakamura, M Yui, and H Mori. Analysis of fifty cases of facial palsy due to otitis media. *Archives of oto-rhino-laryngology*, 241(2):163–168, 1985.

[56] DRAGOSLAV LJ SAVIĆ and DRAGOSLAVA R DJERIĆ. Facial paralysis in chronic suppurative otitis media. *Clinical Otolaryngology & Allied Sciences*, 14(6):515–517, 1989.

[57] Sertac Yetiser, Fuat Tosun, and Mustafa Kazkayas. Facial nerve paralysis due to chronic otitis media. *Otology & neurotology*, 23(4):580–588, 2002.

[58] Brian S Orisek and Richard A Chole. Pressures exerted by experimental cholesteatomas. *Archives of Otolaryngology–Head & Neck Surgery*, 113(4):386–391, 1987.

[59] Glenn Isaacson. Diagnosis of pediatric cholesteatoma. *Pediatrics*, 120(3):603–608, 2007.

[60] Jameel Muzaffar, Christopher Metcalfe, Steve Colley, and Christopher Coulson. Diffusion-weighted magnetic resonance imaging for residual and recurrent cholesteatoma: a systematic review and meta-analysis. *Clinical Otolaryngology*, 42(3):536–543, 2017.

[61] Mark J Syms and William M Luxford. Management of cholesteatoma: status of the canal wall. *The Laryngoscope*, 113(3):443–448, 2003.

[62] Haobing Wang, Clarinda Northrop, Barbara Burgess, M Charles Liberman, and Saumil N Merchant. Three-dimensional virtual model of the human temporal bone: a stand-alone, downloadable teaching tool. *Otology & neurotology: official publication of the American Otological Society, American Neurotology Society [and] European Academy of Otology and Neurotology*, 27(4):452, 2006.

[63] Rong Z Gan, Qunli Sun, Bin Feng, and Mark W Wood. Acoustic–structural coupled finite element analysis for sound transmission in human ear—pressure distributions. *Medical engineering & physics*, 28(5):395–404, 2006.

[64] Rong Z Gan, Brian P Reeves, and Xuelin Wang. Modeling of sound transmission from ear canal to cochlea. *Annals of biomedical engineering*, 35(12):2180–2195, 2007.

[65] Yingxi Liu, Sheng Li, and Xiuzhen Sun. Numerical analysis of ossicular chain lesion of human ear. *Acta Mechanica Sinica*, 25(2):241–247, 2009.

[66] Xiangming Zhang and Rong Z Gan. A comprehensive model of human ear for analysis of implantable hearing devices. *IEEE Transactions on Biomedical Engineering*, 58(10):3024–3027, 2011.

[67] Mads S Sørensen, Andy B Dobrzeniecki, Per Larsen, Thomas Frisch, Jon Sporring, and Tron A Darvann. The visible ear: a digital image library of the temporal bone. *Orl*, 64(6):378–381, 2002.

[68] Haobing Wang, Saumil N Merchant, and Mads S Sorensen. A downloadable three-dimensional virtual model of the visible ear. *ORL*, 69(2):63–67, 2007.

[69] Donaldson J.A. Anson, B.J. The surgical anatomy of the temporal bone and ear. 1976.

[70] Fernanda Gentil, Carolina Garbe, Marco Parente, Pedro Martins, Antonio Ferreira, Renato Natal Jorge, Carla Santos, and Joao Paco. Analysis of eardrum pathologies using the finite element method. *Journal of Mechanics in Medicine and Biology*, 14(03):1450034, 2014.

[71] Bruno Areias, Carla Santos, Renato M Natal Jorge, Fernanda Gentil, and Marco PL Parente. Finite element modelling of sound transmission from outer to inner ear. *Proceedings of the Institution of Mechanical Engineers, Part H: Journal of Engineering in Medicine*, 230(11):999–1007, 2016.

[72] B Areias, MPL Parente, C Santos, Fernanda Gentil, and RM Natal Jorge. The human otitis media with effusion: a numerical-based study. *Computer methods in biomechanics and biomedical engineering*, 20(9):958–966, 2017.

[73] *ABAQUS Analysis User's Manual*, 2019.

[74] Feng B. Sun Q. Gan, R. Z. Three-dimensional finite element modeling of human ear for sound transmission. *Annals of biomedical engineering*, 32(6):847–859, 2004.

[75] T Raveh Tilleman, MM Tilleman, and HAM Neumann. The elastic properties of cancerous skin: Poisson's ratio and young's modulus. *Optimization of Incisions in Cutaneous Surgery including Mohs' Micrographic Surgery.*, page 105, 2004.

[76] Henry Gray. *Anatomy of the human body*, volume 8. Lea & Febiger, 1878.

[77] Guangyao Liu, Qiao Zhang, Yan Jin, and Zhongli Gao. Stress and strain analysis on the anastomosis site sutured with either epineurial or perineurial sutures after simulation of sciatic nerve injury. *Neural regeneration research*, 7(29):2299, 2012.

[78] A Huber, G Ball, M Asai, and R Goode. The vibration pattern of the tympanic membrane after placement of a total ossicular replacement prosthesis. In *Proceeding of the International Workshop on middle ear mechanics in research and otosurgery. Dresden, Germany*, pages 219–222, 1997.

[79] S Nishihara and RL Goode. Measurement of tympanic membrane vibration in 99 human ears. *Middle ear mechanics in research and otosurgery. Dresden University of Technology, Dresden, Germany*, pages 91–93, 1996.

[80] Rong Z Gan, Qunli Sun, Robert K Dyer Jr, Kuang-Hua Chang, and Kenneth J Dormer. Three-dimensional modeling of middle ear biomechanics and its applications. *Otology & Neurotology*, 23(3):271–280, 2002.

[81] Chia-Fone Lee, Peir-Rong Chen, Wen-Jeng Lee, Jyh-Horng Chen, and Tien-Chen Liu. Computer aided three-dimensional reconstruction and modeling of middle ear biomechanics by high-resolution computed tomography and finite element analysis. *Biomedical Engineering: Applications, Basis and Communications*, 18(05):214–221, 2006.